JHEP

Published for SISSA by Springer

Received: July 18, 2018
Revised: November 18, 2018
Accepted: January 22, 2019
Published: February 1, 2019

# Flavor violating Higgs couplings in minimal flavor violation

**Jin-Jun Zhang,**[a] **Min He,**[b] **Xiao-Gang He**[a,b,c,d] **and Xing-Bo Yuan**[c]

[a] *School of Physics and Information Engineering, Shanxi Normal University, Linfen 041004, China*

[b] *Tsung-Dao Lee Institute, and School of Physics and Astronomy, Shanghai Jiao Tong University, Shanghai 200240, China*

[c] *Department of Physics, National Taiwan University, Taipei 10617, Taiwan*

[d] *Physics Division, National Center for Theoretical Sciences, Hsinchu 30013, Taiwan*

*E-mail:* zhangjinjun@sxnu.edu.cn, hemind@sjtu.edu.cn, hexg@phys.ntu.edu.tw, xbyuan@cts.nthu.edu.tw

Abstract: Motivated by the recent LHC data on the lepton-flavor violating (LFV) decays $h \to \ell_1\ell_2$ and $B_{s,d} \to \ell_1\ell_2$, we study the Higgs-mediated flavor-changing neutral current (FCNC) interactions in the effective field theory (EFT) approach without and with the minimal flavor violation (MFV) hypothesis, and concentrate on the later. After considering the $B$ and $K$ physics data, the various LFV processes, and the LHC Higgs data, severe constraints on the Higgs FCNC couplings are derived, which are dominated by the LHC Higgs data, the $B_s - \bar{B}_s$ mixing, and the $\mu \to e\gamma$ decay. In the general case and the MFV framework, allowed ranges of various observables are obtained, such as $\mathcal{B}(B_s \to \ell_1\ell_2)$, $\mathcal{B}(h \to \ell_1\ell_2)$, $\mathcal{B}(h \to q_1q_2)$, and the branching ratio of $\mu \to e$ conversion in Al. Future prospects of searching for the Higgs FCNC interactions at the low-energy experiments and the LHC are discussed.

Keywords: Heavy Quark Physics, Higgs Physics, Beyond Standard Model, CP violation

ArXiv ePrint: 1807.00921



https://doi.org/10.1007/JHEP02(2019)007

JHEP02(2019)007

## Contents


**1 Introduction** **1**

**2 Higgs FCNC couplings** **2**
- 2.1 Higgs FCNC 3
- 2.2 Higgs FCNC in MFV 4

**3 Relevant processes** **7**
- 3.1 Neutral $B$ and $K$ meson mixing 7
- 3.2 $B_s \to \ell_1\ell_2$ decay 8
- 3.3 Leptonic decays $\ell_i \to \ell_j\gamma$ 9
- 3.4 $\mu \to e$ conversion in nuclei 10

**4 Numerical analysis** **11**
- 4.1 Analysis within general Higgs FCNC 13
- 4.2 Analysis in the MFV framework 15

**5 Conclusions** **19**

**A Allowed parameter space in scenario II** **20**


JHEP02(2019)007

## 1 Introduction

The Higgs boson has been discovered at the LHC [1, 2], with a mass of 125 GeV and properties consistent with the standard model (SM) predictions. Precision measurements on the Higgs couplings with the SM particles will be one of the most important tasks for the LHC Run II and its high-luminosity upgrade. A significant deviation from the SM expectations in Higgs phenomenology would be an indicator of new physics (NP) [3, 4].

Besides precision measurements of the Higgs boson at high-energy colliders, it is equally important to search for low-energy processes that are rare or forbidden in the SM [5]. In the SM, the flavor-changing neutral current (FCNC) Yukawa interactions are forbidden at the tree level. However, the Higgs-mediated FCNCs generally appear at the tree level in models beyond the SM [6–9]. These Higgs-mediated couplings can generate the processes which are forbidden in the SM, or enhance some rare decays. In this respect, the lepton-flavor violating (LFV) decays provide excellent probes for such FCNC interactions, such as the $\mu \to e\gamma$, $B_{s,d} \to \ell_1\ell_2$ and $h \to \ell_1\ell_2$ decays ($\ell_{1,2} = e, \mu, \tau$) and can be probed by the LHC and other low energy experiments.

Recently, significant progresses on searching for such interactions are made at the LHC. Based on $3\,\text{fb}^{-1}$ data at Run I, a search for the LFV $B_{s,d}$ decays at the LHCb experiment obtains the following upper limits [10]

$$\mathcal{B}(B_d \to e\mu) < 1.3 \times 10^{-9}\,, \qquad \mathcal{B}(B_s \to e\mu) < 6.3 \times 10^{-9}\,, \tag{1.1}$$

at 95% CL. For the LFV Higgs decays, the CMS collaboration recently provides the best upper bounds [11, 12]

$$\mathcal{B}(h \to e\mu) < 3.5 \times 10^{-4}\,, \quad \mathcal{B}(h \to e\tau) < 6.1 \times 10^{-3}\,, \quad \mathcal{B}(h \to \mu\tau) < 2.5 \times 10^{-3}\,, \tag{1.2}$$

at 95% CL, which have excluded the possibility of sizeable $\mu\tau$ flavor-violating Higgs interactions indicated by the previous CMS measurements [13].

The LFV Higgs couplings can also be indirectly constrained by the lepton FCNC processes, such as the $\mu \to e\gamma$ decay and $\mu \to e$ conversion in nuclei [14, 15]. In the near future, the sensitivity for the branching ratio of $\mu \to e$ conversion in nuclei is expected to be improved by 4 orders of magnitude at the Mu2e experiment, i.e. from $7 \times 10^{-13}$ in Au to $7 \times 10^{-17}$ in Al at 90% CL [16].

It is also noted that, several hints of lepton-flavor universality (LFU) violation emerge in the recent flavor physics data. The current experimental measurements on $R_{K^{(*)}} \equiv \mathcal{B}(B \to K^{(*)}\mu^+\mu^-)/\mathcal{B}(B \to K^{(*)}e^+e^-)$ and $R_{D^{(*)}} = \mathcal{B}(B \to D^{(*)}\tau\nu)/\mathcal{B}(B \to D^{(*)}\ell\nu)$ show about $2\sigma$ [17, 18] and $4\sigma$ [19] deviations from their SM predictions, respectively. Although such anomalies may not be related to the Higgs FCNC interactions directly, the NP candidates to explain these anomalies sometimes involve the Higgs FCNC couplings [20–24].

In this work, motivated by these recent progresses and future prospects, we study the Higgs-mediated FCNC effects on various processes. We adopt an effective field theory (EFT) approach, in which the Higgs FCNC interactions are described by dim-6 operators [5]. In this approach, some FCNC couplings are severely constrained from flavor physics. In order to naturally obtain such small couplings, we concentrate on the minimal flavor violation hypothesis (MFV) [25–27] as a particular working assumption. After deriving direct and indirect bounds on the Higgs FCNC couplings, we discuss in detail the future prospects of searching for these FCNC interactions in various processes.

This paper is organized as follows: in section 2, we give a brief overview of the tree-level Higgs FCNC couplings in the EFT with and without the MFV hypothesis. In section 3, we discuss their effects on various flavor processes. In section 4, we present our detailed numerical results and discussions. Our conclusions are given in section 5.

## 2 Higgs FCNC couplings

The Higgs FCNC Yukawa couplings appear in many extensions of the SM in the Higgs sector, such as multi-Higgs doublet models. In this work, we will not go into detailed model studies of these FCNC couplings but adopt an EFT approach to use known data to obtain model independent constraints on them. The framework that will be used for the analysis of the Higgs FCNC couplings in the EFT approach and a special form in the MFV framework will be provided in the following.



JHEP02(2019)007

### 2.1 Higgs FCNC

In the SM, the Yukawa interactions with quarks are described by the following Lagrangian in the interaction basis,

$$-\mathcal{L}_Y = \bar{Q}_L H Y_d d_R + \bar{Q}_L \tilde{H} Y_u u_R + \text{h.c.}, \tag{2.1}$$

where $Q_L$ denotes the left-handed quark doublet, $d_R$ the right-handed down-type quarks, $u_R$ the right-handed up-type quarks, $H$ the Higgs doublet, and $\tilde{H} \equiv i\sigma_2 H^*$. The Yukawa coupling matrices $Y_{u,d}$ are $3 \times 3$ complex matrices in flavor space.

In the SM, the Higgs doublet develops a non-zero vacuum expectation value $\langle H \rangle = v/\sqrt{2}$ which breaks electroweak weak symmetry down to $\text{U}(1)_{\text{em}}$, the charged Higgs fields $H^\pm$ and the imaginary part of the neutral components are "eaten" by $W^\pm$ and $Z$ bosons and left a physical neutral Higgs $h$. Working in the basis of quark mass eigenstates, the above Lagrangian gives a flavor conserving Higgs-fermion coupling of the form $m_f \bar{f} f(1 + h/v)$.

When going beyond the SM, the above simple flavor conserving couplings will be modified. Considering the BSM effects in the EFT approach, these Higgs Yukawa interactions can be affected by dim-6 operators at the tree level. There are several different bases to choose for writing down the operators. We will work in the Warsaw basis in ref. [28]. There exist only three operators relevant to our analysis to the lowest order. They are given by

$$\begin{aligned} \mathcal{O}_{dH} &= (H^\dagger H)(\bar{Q}_L H C_{dH} d_R), \\ \mathcal{O}_{uH} &= (H^\dagger H)(\bar{Q}_L \tilde{H} C_{uH} u_R), \\ \mathcal{O}_{\ell H} &= (H^\dagger H)(\bar{L}_L H C_{\ell H} e_R), \end{aligned} \tag{2.2}$$

where the doublet/singlet $Q_L$, $u_R$, $d_R$, and the couplings $C_{uH,dH,\ell H}$ are in flavour space, and their flavour indices are omitted. It is also noted that these operators can arise in many BSM scenarios, such as Extra Dimensions [29, 30], Composite Higgs [31, 32], models with vector-like quarks [33], Two-Higgs Doublet Models [34, 35], and other extended Higgs sectors [36]. In a genuine EFT approach, analysis of low-energy flavor transitions, such as $B_s - \bar{B}_s$ mixing, should include not only the operators listed in eq. (2.2), but also other dim-6 operators which can affect these flavor transitions at the tree level. In the Warsaw basis, these additional operators are 4-fermion operators, such as $(\bar{Q}_L \gamma_\mu Q_L)(\bar{Q}_L \gamma^\mu Q_L)$, dipole operators, such as $(\bar{Q}_L \sigma^{\mu\nu} d_R) H B_{\mu\nu}$, and operators involving $(H^\dagger i \overleftrightarrow{D}_\mu H)$, such as $(H^\dagger i \overleftrightarrow{D}_\mu H)(\bar{Q}_L \gamma^\mu Q_L)$. It is noted that all these operators do not contribute to the Higgs FCNC Yukawa couplings at the tree level. Therefore, in this work, we don't consider these operators and their effects to the low-energy FCNC processes are assumed to be negligible compared to the contributions from the Higgs FCNC Yukawa couplings. Our numerical results in section 4 are valid only under this assumption. We refer to refs. [38] and [39, 40] for general EFT analysis of $B$-meson FCNC processes and $\mu \to e$ transitions, respectively.

The assumption that the BSM contributions to the low-energy flavour transitions are dominated by the effect of the modified Higgs Yukawa couplings in the form of eq. (2.2) has limitation in EFT analysis. For example, in the type-II 2HDM, a tree-level matching gives the effective Lagrangian $\Delta\mathcal{L}_{\text{eff}} = (1/\Lambda^2)[2Z_6(\eta_f/\tan\beta) H^\dagger H \bar{f}_R Y_f f_L H +$



JHEP02(2019)007

$(\eta_f/\tan\beta)^2(\bar{f}_L Y_f f_R)(\bar{f}_L Y_f f_R)]$. Here, $Z_6$ is the coefficient of $|H_1|^2(H_1^\dagger H_2)$ in the scalar potential, $\Lambda$ denotes the mass scale of $m_A$, $m_{H^\pm}$ and $m_{H^0}$, $\eta_u = 1$, and $\eta_d = -\tan^2\beta$ [34]. Therefore, in the processes involving four down-type fermions, e.g., $\bar{s}s\bar{d}d$, the condition for the effect of modified Yukawa couplings dominates over the one of four-fermion operator is $Z_6 v^2/m_h^2 \gg \tan\beta$, which requires a large $Z_6$ or small $\tan\beta$. However, these parameter space are disfavored by the combined constraints of the Electro-Weak Precision Test, the current LHC Higgs data, and flavour physics. The situation in the Composite Higgs models is different. In the Composite Higgs scenario in ref. [37], a Naive Dimension Analysis (NDA) gives that the Wilson coefficients of the low-energy $\Delta F = 2$ FCNC four-fermion operators from the Higgs, $Z$ and heavy vector exchange have the power counting $C_{\rm Higgs} : C_Z : C_{\rm HV} \sim (y_*^2/m_h^2)(y_*^2 v^2/\Lambda^2)^2 : (g_2^2/m_Z^2)(g_*^2 v^2/\Lambda^2)^2 : (g_*^2/\Lambda^2)$. Here $y_*$ and $g_*$ denote the typical coupling of the composite Higgs to the other strong states and the typical coupling of the heavy resonances of the strong sector, respectively. In the parameter region $y_*^6(v^4/m_h^2\Lambda^2) \gg g_*^2$, the contribution from the Higgs exchange is dominant.

The operators above can contribute to the fermion mass terms in dim-4 $\mathcal{L}_{\rm SM}$ after the symmetry breaking $H^\dagger H \to 1/2v^2$. The Yukawa couplings of $h$ to fermions are given by

$$\mathcal{L}_Y^f = -\frac{1}{\sqrt{2}}\bar{f}_L \bar{Y}_f f_R v - \frac{1}{\sqrt{2}}\bar{f}_L\left(\bar{Y}_f - \frac{v^2}{\Lambda^2}C_{fH}\right) f_R h + \text{h.c.}, \tag{2.3}$$

with the definition

$$\bar{Y}_f = Y_f - \frac{1}{2}\frac{v^2}{\Lambda^2}C_{fH}, \tag{2.4}$$

where $\Lambda$ denotes some NP scale.

In the mass-eigenstate basis $\bar{Y}_f$ becomes diagonal, but the Higgs Yukawa interactions $(1/\sqrt{2})(\bar{Y}_f - (v^2/\Lambda^2)C_{fH})$ is in general not diagonal [41] and induces FCNC interactions. We write them as

$$\mathcal{L}_Y = -\frac{1}{\sqrt{2}}\bar{f}(Y_L P_L + Y_R P_R) f h, \tag{2.5}$$

Where $f$ denotes $(u, c, t)$, $(d, s, b)$ or $(e, \mu, \tau)$. $Y_L$ and $Y_R$ are $3 \times 3$ complex matrices in flavor space and connect to each other by the relation $Y_L = Y_R^\dagger$. In the SM, $Y_R^u = Y_f$ is diagonalized to have $\lambda_u^i = \sqrt{2}m_i/v$ and the vacuum expectation value $v = 246\,\text{GeV}$. Now $\bar{Y}_u$ plays the role of $Y_u$. Similarly for $d$ and $\ell$ sectors. Here we have used dim-6 operators to show how to parametrize the general form of a Higgs to fermions couplings. This should apply to more general cases.

In the literature, the following basis for the Higgs Yukawa interactions is also widely used

$$\mathcal{L}_Y = -\frac{1}{\sqrt{2}}\bar{f}(Y + i\gamma_5\bar{Y}) f h\,. \tag{2.6}$$

Here, $Y$ and $\bar{Y}$ are $3 \times 3$ Hermitian matrices. This form is related to eq. (2.5) by $Y_{R,L} = Y \pm i\bar{Y}$. It is noted that real $Y_{L,R}^{ij}$ do not imply real $Y_{ij}$ or $\bar{Y}_{ij}$, and *vice versa*.

### 2.2 Higgs FCNC in MFV

In the SM, the Yukawa interactions in eq. (2.1) violate the global flavor symmetry

$$G_{\rm QF} = \text{SU}(3)_{Q_L} \otimes \text{SU}(3)_{u_R} \otimes \text{SU}(3)_{d_R}\,. \tag{2.7}$$



JHEP02(2019)007

This flavor symmetry can be recovered by formally promoting the Yukawa matrices to spurions fields, which transform as

$$Y_u \sim (\mathbf{3}, \bar{\mathbf{3}}, \mathbf{1}) \qquad \text{and} \qquad Y_d \sim (\mathbf{3}, \mathbf{1}, \bar{\mathbf{3}}). \tag{2.8}$$

Then, two basic building block spurions $\mathsf{A} \equiv Y_u Y_u^\dagger$ and $\mathsf{B} \equiv Y_d Y_d^\dagger$ under the group $\mathrm{SU}(3)_{Q_L} \otimes \mathrm{SU}(3)_{u_R} \otimes \mathrm{SU}(3)_{d_R}$ transforming as $(\mathbf{1}+\mathbf{8}, \mathbf{1}, \mathbf{1})$ are important to parametrize the FCNC Yukawa couplings.

The coefficients $C_{uH,dH}$ in eq. (2.3) are in general independent from the tree level defined Yukawa couplings $Y_{u,d}$. To have more definitive framework for our later analysis, we will work under the assumption of MFV hypothesis. This hypothesis implies that [27], all CP and flavor violating sources come from $Y_{u,d}$ and the effective Lagrangian is invariant under the flavor symmetry group $G_{\mathrm{QF}}$. Therefore $C_{uH,dH}$ can be written in the following form in order to have the right transformation properties under $G_{\mathrm{QF}}$,

$$C_{dH} = f_d(\mathsf{A}, \mathsf{B}) Y_d \quad \text{and} \quad C_{uH} = f_u(\mathsf{A}, \mathsf{B}) Y_u \,. \tag{2.9}$$

The function $f_{u,d}(\mathsf{A}, \mathsf{B})$ can be expanded in an infinite series of the form $f_{u,d}(\mathsf{A}, \mathsf{B}) \equiv \xi^{u,d}_{ijk\cdots} \mathsf{A}^i \mathsf{B}^j \mathsf{A}^k \cdots$ with $\xi^{u,d}_{ijk\cdots}$ to be real since no new CP violating source should be introduced other than that already contained in $Y_{u,d}$. Using the Cayley-Hamilton identity, $f(\mathsf{A}, \mathsf{B})$ can be generally resumed into 17 terms [42, 43],

$$\begin{aligned} f(\mathsf{A}, \mathsf{B}) = {} & \kappa_1 \mathbb{1} + \kappa_2 \mathsf{A} + \kappa_5 \mathsf{B}^2 + \kappa_6 \mathsf{A}\mathsf{B} + \kappa_8 \mathsf{A}\mathsf{B}\mathsf{A} + \kappa_{11} \mathsf{A}\mathsf{B}^2 + \kappa_{13} \mathsf{A}^2\mathsf{B}^2 + \kappa_{15} \mathsf{B}^2\mathsf{A}\mathsf{B} + \kappa_{16} \mathsf{A}\mathsf{B}^2\mathsf{A}^2 \\ & + \kappa_3 \mathsf{B} + \kappa_4 \mathsf{A}^2 + \kappa_7 \mathsf{B}\mathsf{A} + \kappa_{10} \mathsf{B}\mathsf{A}\mathsf{B} + \kappa_9 \mathsf{B}\mathsf{A}^2 + \kappa_{14} \mathsf{B}^2\mathsf{A}^2 + \kappa_{12} \mathsf{A}\mathsf{B}\mathsf{A}^2 + \kappa_{17} \mathsf{B}^2\mathsf{A}^2\mathsf{B} \,. \end{aligned}$$

Due to the resummation, the coefficients $\kappa_i$ can receive some contributions from combinations of $\mathsf{A}$ and $\mathsf{B}$ and become complex generally. However, it can be shown that $\mathrm{Im}\kappa_i \propto |\mathrm{Tr}(\mathsf{A}^2\mathsf{B}\mathsf{A}\mathsf{B}^2)| \ll 1$ and therefore these tiny imaginary parts can be neglected in our numerical analysis [42–46]. Since the spurion $\mathsf{B}$ is highly suppressed by the small down-type quark Yukawa couplings, terms with $\mathsf{B}$ are neglected and we obtain [47]

$$f_u(\mathsf{A}, \mathsf{B}) \approx \epsilon_0^u \mathbb{1} + \epsilon_1^u \mathsf{A} + \epsilon_2^u \mathsf{A}^2 \quad \text{and} \quad f_d(\mathsf{A}, \mathsf{B}) \approx \epsilon_0^d \mathbb{1} + \epsilon_1^d \mathsf{A} + \epsilon_2^d \mathsf{A}^2 \,. \tag{2.10}$$

The coefficients $\epsilon^u_{0,1,2}$ and $\epsilon^d_{0,1,2}$ are free complex parameters but have negligible imaginary components [42–46].

For the down-type quarks, the Yukawa interactions with the dim-6 operator $\mathcal{O}_{dH}$ after the EW symmetry breaking read

$$\mathcal{L}_Y^d = -\frac{1}{\sqrt{2}} \bar{d}_L \bar{Y}_d d_R v - \frac{1}{\sqrt{2}} \bar{d}_L \left( \bar{Y}_d - \frac{v^2}{\Lambda^2} C_{dH} \right) d_R h + \text{h.c.} \,. \tag{2.11}$$

with the definition

$$\bar{Y}_f = Y_f - \frac{1}{2} \frac{v^2}{\Lambda^2} C_{fH} \,. \tag{2.12}$$

Using the MFV hypothesis in eq. (2.9) and the approximation in eq. (2.10),

$$C_{dH} = \left[ \epsilon_0^d \mathbb{1} + \epsilon_1^d Y_u Y_u^\dagger + \epsilon_2^d (Y_u Y_u^\dagger)^2 \right] Y_d \,. \tag{2.13}$$



JHEP02(2019)007

With the redefinition in eq. (2.12)

$$C_{dH} = \left[\epsilon_0^d \mathbb{1} + \epsilon_1^d \bar{Y}_u \bar{Y}_u^\dagger + \epsilon_2^d (\bar{Y}_u \bar{Y}_u^\dagger)^2\right] \bar{Y}_d + \mathcal{O}(v^2/\Lambda^2)\,. \tag{2.14}$$

Finally, we obtain the Yukawa interactions for down-type quarks in the mass eigenstate

$$\mathcal{L}_Y^d = -\frac{1}{\sqrt{2}} \bar{d}_L \left[(1-\hat{\epsilon}_0^d)\lambda_d - \hat{\epsilon}_1^d V^\dagger \lambda_u^2 V \lambda_d - \hat{\epsilon}_2^d V^\dagger \lambda_u^4 V \lambda_d\right] d_R h + \text{h.c.}\,, \tag{2.15}$$

with the definition $\hat{\epsilon}_i^d = (v^2/\Lambda^2)\epsilon_i^d$. Due to the large hierarchy in the diagonal matrix $\lambda_u$, the $\hat{\epsilon}_1^d$ and $\hat{\epsilon}_2^d$ terms have almost the same structure. Therefore, we will use the following approximation in the numerical analysis

$$\mathcal{L}_Y^d = -\frac{1}{\sqrt{2}} \bar{d}_L \left[(1-\hat{\epsilon}_0^d)\lambda_d - \hat{\epsilon}_1^d V^\dagger \lambda_u^2 V \lambda_d\right] d_R h + \text{h.c.}\,, \tag{2.16}$$

which is equivalent to redefine $(\hat{\epsilon}_1^d + \lambda_t^2 \hat{\epsilon}_2^d) \to \hat{\epsilon}_1^d$. We have checked that the numerical differences due to this approximation are negligible.

Similarly, the Yukawa interactions for up-type quarks in the MFV are obtained

$$\mathcal{L}_Y^u = -\frac{1}{\sqrt{2}} \bar{u}_L \left[(1-\hat{\epsilon}_0^u)\lambda_u - \hat{\epsilon}_1^u \lambda_u^3 - \hat{\epsilon}_2^u \lambda_u^5\right] u_R h + \text{h.c.}\,, \tag{2.17}$$

with the definition $\hat{\epsilon}_i^u = (v^2/\Lambda^2)\epsilon_i^u$. Due to the large hierarchy in the diagonal matrix $\lambda_u$ and $\lambda_t \approx 1$, we take the approximation $\hat{\epsilon}_0^u \lambda_u + \hat{\epsilon}_1^u \lambda_u^3 + \hat{\epsilon}_2^u \lambda_u^5 \approx (\hat{\epsilon}_0^u + \hat{\epsilon}_1^u + \hat{\epsilon}_2^u)\lambda_u$. Finally, after a redefinition $(\hat{\epsilon}_0^u + \hat{\epsilon}_1^u + \hat{\epsilon}_2^u) \to \hat{\epsilon}_0^u$, the following Lagrangian for up-type quarks are obtained

$$\mathcal{L}_Y^u = -\frac{1}{\sqrt{2}} \bar{u}_L (1-\hat{\epsilon}_0^u)\lambda_u u_R h + \text{h.c.}\,. \tag{2.18}$$

We have checked that the numerical differences due to this approximation are negligible. In the MFV, the FCNC in the up sector is negligibly small.

For the lepton sector, definition of MFV depends on the underlying mechanism responsible for neutrino masses and is not unique [48–51]. Here, we adopt the approach in ref. [47], which is based on type-I seesaw mechanism. Then, the basic building block spurion similar to $\mathsf{A}$ in the quark sector, reads in the mass eigenstate

$$\mathsf{A}_\ell = \frac{2\mathcal{M}}{v^2} U \hat{m}_\nu^{1/2} O O^\dagger \hat{m}_\nu^{1/2} U^\dagger\,, \tag{2.19}$$

where $U$ denotes the Pontecorvo-Maki-Nakagawa-Sakata matrix, $\hat{m}_\nu$ the diagonal neutrino mass matrix $\text{diag}(m_1, m_2, m_3)$ and $\mathcal{M}$ mass of the right-handed neutrinos. Matrix $O$ is generally complex orthogonal, satisfying $OO^T = \mathbb{1}$ [52]. Then, after neglecting small $\mathsf{B}_\ell$ terms, the Yukawa interactions for charged lepton reads

$$\mathcal{L}_Y^\ell = -\frac{1}{\sqrt{2}} \bar{\ell}_L \left[(1-\hat{\epsilon}_0^\ell)\lambda_\ell - \hat{\epsilon}_1^\ell \mathsf{A}_\ell \lambda_\ell - \hat{\epsilon}_2^\ell \mathsf{A}_\ell^2 \lambda_\ell\right] \ell_R h\,, \tag{2.20}$$

with the definition $\hat{\epsilon}_i^\ell = (v^2/\Lambda^2)\epsilon_i^\ell$.



JHEP02(2019)007

In summary, the Yukawa couplings in the MFV framework can be written as in the basis of eq. (2.5),

$$\begin{aligned} Y_R^d &= (1-\hat{\epsilon}_0^d)\lambda_d - \hat{\epsilon}_1^d V^\dagger \lambda_u^2 V \lambda_d \,, \\ Y_R^u &= (1-\hat{\epsilon}_0^u)\lambda_u \,, \\ Y_R^\ell &= (1-\hat{\epsilon}_0^\ell)\lambda_\ell - \hat{\epsilon}_1^\ell \mathsf{A}_\ell \lambda_\ell - \hat{\epsilon}_2^\ell \mathsf{A}_\ell^2 \lambda_\ell . \end{aligned} \tag{2.21}$$

All the above Yukawa matrices are Hermitian in the MFV framework.

## 3 Relevant processes

In this section we consider possible processes which can constrain the Higgs FCNC couplings to fermions. We find the most relevant processes are $B_s - \bar{B}_s$, $B_d - \bar{B}_d$ and $K^0 - \bar{K}^0$ mixing, $B_{s,d} \to \ell_1 \ell_2$ decays, the leptonic decays $\ell_i \to \ell_j \gamma$ and $\mu \to e$ conversion in nuclei, and Higgs production and decay at the LHC, which are investigated in detail in this section.

### 3.1 Neutral $B$ and $K$ meson mixing

Including the Higgs FCNC contributions, the effective Hamiltonian for $B_s - \bar{B}_s$ mixing can be written as [53]

$$\mathcal{H}_{\rm eff}^{\Delta B=2} = \frac{G_F^2}{16\pi^2} m_W^2 (V_{tb}V_{ts}^*)^2 \sum_i C_i \mathcal{O}_i + \text{h.c.} \,, \tag{3.1}$$

where the operators relevant to our study are

$$\begin{aligned} \mathcal{O}_1^{\rm VLL} &= (\bar{s}^\alpha \gamma_\mu P_L b^\alpha)(\bar{s}^\beta \gamma^\mu P_L b^\beta) \,, & \mathcal{O}_1^{\rm SLL} &= (\bar{s}^\alpha P_L b^\alpha)(\bar{s}^\beta P_L b^\beta) \,, \\ \mathcal{O}_2^{\rm LR} &= (\bar{s}^\alpha P_L b^\alpha)(\bar{s}^\beta P_R b^\beta) \,, & \mathcal{O}_1^{\rm SRR} &= (\bar{s}^\alpha P_R b^\alpha)(\bar{s}^\beta P_R b^\beta) \,, \end{aligned} \tag{3.2}$$

with $\alpha$ and $\beta$ color indices. $V_{ij}$ denote the Cabibbo-Kobayashi-Maskawa (CKM) matrix elements. The SM contributes to only the $\mathcal{O}_1^{\rm VLL}$ operator, whose Wilson coefficients $C_1^{\rm VLL}$ can be found in ref. [54]. The other operators can be generated by tree-level Higgs FCNC exchange, whose Wilson coefficients read [41]

$$\begin{aligned} C_1^{\rm SLL,NP} &= -\frac{1}{2}\tilde{\kappa}\big(Y_L^{sb}\big)^2 \,, & C_2^{\rm LR,NP} &= -\tilde{\kappa} Y_L^{sb} Y_R^{sb} \,, \\ C_1^{\rm SRR,NP} &= -\frac{1}{2}\tilde{\kappa}\big(Y_R^{sb}\big)^2 \,, & \tilde{\kappa} &= \frac{8\pi^2}{G_F^2}\frac{1}{m_h^2 m_W^2}\frac{1}{(V_{tb}V_{ts}^*)^2} \,. \end{aligned} \tag{3.3}$$

The contribution from $\mathcal{H}_{\rm eff}^{\Delta B=2}$ to the transition matrix element of $B_s - \bar{B}_s$ mixing is given by [53],

$$M_{12}^s = \langle B_s | \mathcal{H}_{\rm eff}^{\Delta B=2} | \bar{B}_s \rangle = \frac{G_F^2}{16\pi^2} m_W^2 (V_{tb}V_{ts}^*)^2 \sum C_i \langle B_s | \mathcal{O}_i | \bar{B}_s \rangle \,, \tag{3.4}$$

where recent lattice calculations of the hadronic matrix elements $\langle \mathcal{O}_i \rangle$ can be found in refs. [55, 56]. Then the mass difference and CP violation phase read

$$\Delta m_s = 2|M_{12}^s| \,, \qquad \text{and} \qquad \phi_s = \arg M_{12}^s \,. \tag{3.5}$$



JHEP02(2019)007

In the case of complex Yukawa couplings, $\phi_s$ can deviate from the SM prediction, i.e., $\phi_s = \phi_s^{\rm SM} + \phi_s^{\rm NP}$. Nonzero $\phi_s^{\rm NP}$ can affect the CP violation in the $B_s \to J/\psi\phi$ decay [57], as well as $\mathcal{A}_{\Delta\Gamma}$ in the $B_s \to \mu^+\mu^-$ decay as in eq. (3.14). In the basis in eq. (2.6), it can be seen that the mass difference $\Delta m_s$ depends only on $Y_{sb}^2$ and $\bar{Y}_{sb}^2$, but not $Y_{sb}\bar{Y}_{sb}$. In addition, we follow ref. [53] to perform renormalization group evolution of the NP operators $\mathcal{O}_1^{\rm SLL}$, $\mathcal{O}_1^{\rm SRR}$ and $\mathcal{O}_2^{\rm LR}$. It is found that including RG effects of the NP operators enhances the NP contributions by about a factor of 2.

### 3.2 $B_s \to \ell_1\ell_2$ decay

In this subsection, we consider the $B_s \to \mu^+\mu^-$ decay as an example to recapitulate the theoretical framework of the $B_s \to \ell_1\ell_2$ processes. Within the Higgs FCNC effects, the effective Hamiltonian of the $B_s \to \mu^+\mu^-$ decay reads [54]

$$\mathcal{H}_{\rm eff} = -\frac{G_F}{\sqrt{2}}\frac{\alpha_e}{\pi s_W^2} V_{tb}V_{ts}^* \big(C_A\mathcal{O}_A + C_S\mathcal{O}_S + C_P\mathcal{O}_P + C_S'\mathcal{O}_S' + C_P'\mathcal{O}_P'\big) + \text{h.c.}, \tag{3.6}$$

where $\alpha_e$ is the fine structure constant, and $s_W^2 \equiv \sin^2\theta_W$ with $\theta_W$ being the weak mixing angle. The operators $\mathcal{O}_i^{(\prime)}$ are defined as

$$\begin{aligned} \mathcal{O}_A &= \big(\bar{q}\gamma_\mu P_L b\big)\big(\bar{\mu}\gamma^\mu\gamma_5\mu\big)\,, \quad & \mathcal{O}_S &= m_b\big(\bar{q}P_R b\big)\big(\bar{\mu}\mu\big)\,, \quad & \mathcal{O}_P &= m_b\big(\bar{q}P_R b\big)\big(\bar{\mu}\gamma_5\mu\big)\,, \\ & & \mathcal{O}_S' &= m_b\big(\bar{q}P_L b\big)\big(\bar{\mu}\mu\big)\,, \quad & \mathcal{O}_P' &= m_b\big(\bar{q}P_L b\big)\big(\bar{\mu}\gamma_5\mu\big)\,. \end{aligned} \tag{3.7}$$

In the framework we are working with, the Wilson coefficient $C_A$ contains only the SM contribution, and its explicit expression up to the NLO QCD corrections can be found in refs. [58–60]. Recently, corrections at the NLO EW [61] and NNLO QCD [62] have been completed, with the numerical value approximated by [63]

$$C_A^{\rm SM}(\mu_b) = -0.4690\left(\frac{m_t^{\rm P}}{173.1\ \text{GeV}}\right)^{1.53}\left(\frac{\alpha_s(m_Z)}{0.1184}\right)^{-0.09}\,, \tag{3.8}$$

where $m_t^{\rm P}$ denotes the top-quark pole mass. In the SM, the Wilson coefficients $C_S^{\rm SM}$ and $C_P^{\rm SM}$ can be induced by the Higgs-penguin diagrams but are highly suppressed. Their expressions can be found in refs. [64, 65]. As a very good approximation, we can safely take $C_S^{\rm SM} = C_S'^{\rm SM} = C_P^{\rm SM} = C_P'^{\rm SM} = 0$.

With the Higgs-mediated FCNC interactions in the effective Lagrangian, eq. (2.5), the scalar and pseudoscalar Wilson coefficients read

$$\begin{aligned} C_S^{\rm NP} &= \frac{1}{2}\kappa Y_R^{sb}\big(Y_R^{\mu\mu} + Y_L^{\mu\mu}\big)\,, \quad & C_P^{\rm NP} &= \frac{1}{2}\kappa Y_R^{sb}\big(Y_R^{\mu\mu} - Y_L^{\mu\mu}\big)\,, \\ C_S'^{\rm NP} &= \frac{1}{2}\kappa Y_L^{sb}\big(Y_R^{\mu\mu} + Y_L^{\mu\mu}\big)\,, \quad & C_P'^{\rm NP} &= \frac{1}{2}\kappa Y_L^{sb}\big(Y_R^{\mu\mu} - Y_L^{\mu\mu}\big)\,, \end{aligned} \tag{3.9}$$

with the common factor

$$\kappa = \frac{\pi^2}{2G_F^2}\frac{1}{V_{tb}V_{ts}^*}\frac{1}{m_b m_h^2 m_W^2}\,. \tag{3.10}$$



JHEP02(2019)007

For the effective Hamiltonian eq. (3.6), the branching ratio of $B_s \to \mu^+\mu^-$ reads [64, 65]

$$\mathcal{B}(B_s \to \mu^+\mu^-) = \frac{\tau_{B_s} G_F^4 m_W^4}{8\pi^5} |V_{tb}V_{ts}^*|^2 f_{B_s}^2 m_{B_s} m_\mu^2 \sqrt{1-\frac{4m_\mu^2}{m_{B_s}^2}} \left(|P|^2 + |S|^2\right) , \tag{3.11}$$

where $m_{B_s}$, $\tau_{B_s}$ and $f_{B_s}$ denote the mass, lifetime and decay constant of the $B_s$ meson, respectively. The amplitudes $P$ and $S$ are defined as

$$\begin{aligned} P &\equiv C_A + \frac{m_{B_s}^2}{2m_\mu} \left(\frac{m_b}{m_b+m_s}\right) (C_P - C_P') , \\ S &\equiv \sqrt{1-\frac{4m_\mu^2}{m_{B_s}^2}} \frac{m_{B_s}^2}{2m_\mu} \left(\frac{m_b}{m_b+m_s}\right) (C_S - C_S') . \end{aligned} \tag{3.12}$$

From these expressions and using the basis in eq. (2.6), it can be seen that the branching ratio of $B_s \to \mu^+\mu^-$ only depends on $\bar{Y}_{sb}Y_{\mu\mu}$ and $\bar{Y}_{sb}\bar{Y}_{\mu\mu}$.

Due to the $B_s$-$\bar{B}_s$ oscillations, the measured branching ratio of $B_s \to \mu^+\mu^-$ should be the time-integrated one [66]:

$$\bar{\mathcal{B}}(B_s \to \mu^+\mu^-) = \left(\frac{1+\mathcal{A}_{\Delta\Gamma} y_s}{1-y_s^2}\right) \mathcal{B}(B_s \to \mu^+\mu^-) , \tag{3.13}$$

with [67]

$$y_s = \frac{\Gamma_s^{\rm L} - \Gamma_s^{\rm H}}{\Gamma_s^{\rm L} + \Gamma_s^{\rm H}} = \frac{\Delta\Gamma_s}{2\Gamma_s} \quad \text{and} \quad \mathcal{A}_{\Delta\Gamma} = \frac{|P|^2\cos\left(2\varphi_P - \phi_s^{\rm NP}\right) - |S|^2\cos\left(2\varphi_S - \phi_s^{\rm NP}\right)}{|P|^2 + |S|^2} , \tag{3.14}$$

Here, $\Gamma_s^{\rm L}$ ($\Gamma_s^{\rm H}$) denote the decay widths of the light (heavy) $B_s$ mass eigenstates. $\varphi_P$ and $\varphi_S$ are the phases associated with $P$ and $S$, respectively. The CP phase $\phi_s^{\rm NP}$ comes from $B_s$-$\bar{B}_s$ mixing and has been defined in eq. (3.5). In the SM, $\mathcal{A}_{\Delta\Gamma}^{\rm SM} = 1$.

### 3.3 Leptonic decays $\ell_i \to \ell_j\gamma$

Considering the Higgs FCNC interactions, the effective Lagrangian for the $\ell_i \to \ell_j\gamma$ decays are given by [5]

$$\mathcal{L}_{\rm eff} = c_L\mathcal{O}_L + c_R\mathcal{O}_R + \text{h.c.}, \tag{3.15}$$

with the operators

$$\mathcal{O}_{L,R} = \frac{e}{8\pi^2} m_i (\bar{\ell}_j \sigma^{\mu\nu} P_{L,R} \ell_i) F_{\mu\nu} , \tag{3.16}$$

where $m_i$ denotes the mass of the lepton $\ell_i$ and $F_{\mu\nu}$ the photon field strength tensor. Then, the decay rate of $\ell_i \to \ell_j\gamma$ is given by [5]

$$\Gamma(\ell_i \to \ell_j\gamma) = \frac{\alpha_e m_i^5}{64\pi^4} (|c_L|^2 + |c_R|^2). \tag{3.17}$$

The Wilson coefficients $c_L$ and $c_R$ receive contributions from the one-loop penguin diagrams. Their analytical expressions read [5]

$$c_L^{\rm 1-loop} = \sum_{f=e,\mu,\tau} F(m_i, m_f, m_j, 0, Y), \qquad c_R^{\rm 1-loop} = \sum_{f=e,\mu,\tau} F(m_i, m_f, m_j, 0, Y^\dagger), \tag{3.18}$$



JHEP02(2019)007

with the loop function

$$F(m_i,m_f,m_j,q^2,Y)=\frac{1}{8m_i}\int_0^1 dxdydz\delta(1-x-y-z)\\ \times\frac{xzm_jY_R^{jf}Y_L^{fi}+yzm_iY_L^{jf}Y_R^{fi}+(x+y)m_fY_L^{jf}Y_L^{fi}}{zm_h^2-xzm_j^2-yzm_i^2+(x+y)m_f^2-xyq^2}.$$

At the two-loop level, there are also comparable contributions from the Barr-Zee type diagrams. Here, we use the numerical results in ref. [5].

$$c_L^{2-\text{loop}}\approx\frac{1}{\sqrt{2}m_h^2}\frac{m_\tau}{m_i}Y_L^{ji}(-0.058Y_R^{tt}+0.11),\\ c_R^{2-\text{loop}}\approx\frac{1}{\sqrt{2}m_h^2}\frac{m_\tau}{m_i}Y_R^{ji}(-0.058Y_L^{tt}+0.11),\tag{3.19}$$

which are obtained from a full two-loop analytical calculations [68]. Here, $Y_L^{tt}$ and $Y_R^{tt}$ are assumed to be real.

### 3.4 $\mu\to e$ conversion in nuclei

The Higgs FCNC interactions could induce $\mu\to e$ conversion in nuclei. The relevant effective Lagrangian reads [5]

$$\mathcal{L}_{\text{eff}}=c_L\frac{e}{8\pi^2}m_\mu(\bar{e}\sigma^{\mu\nu}P_L\mu)F_{\mu\nu}-\frac{1}{2}\sum_q\Big[g_{LS}^q(\bar{e}P_R\mu)(\bar{q}q)+g_{LV}^q(\bar{e}\gamma^\mu P_L\mu)(\bar{q}\gamma_\mu q)\Big]+\big(L\leftrightarrow R\big),\tag{3.20}$$

where the summation runs over all quark flavors $q\in\{u,d,s,c,b,t\}$. The Wilson coefficients $c_{L,R}$ are the same with the ones in $\mu\to e\gamma$ in eq. (3.15). The scalar operators are generated by the tree-level Higgs exchange and their Wilson coefficients are given by

$$g_{LS}^q=-\frac{1}{m_h^2}Y_R^{e\mu}\text{Re}(Y_R^{qq}),\qquad g_{RS}^q=-\frac{1}{m_h^2}Y_L^{e\mu}\text{Re}(Y_R^{qq}).\tag{3.21}$$

For the vector operators, the leading contributions arise from one-loop penguin diagrams, and the corresponding Wilson coefficients read [5]

$$g_{LV}^q=-\frac{\alpha_eQ_q}{2\pi q^2}\sum_{f=e,\mu,\tau}[G(m_\mu,m_f,m_e,q^2,Y)-G(m_\mu,m_f,m_e,0,Y)],\tag{3.22}$$

with the loop function

$$G(m_i,m_f,m_j,q^2,Y)=\frac{1}{2}\int_0^1dx\int_0^{1-x}dy\Big\{+Y_R^{jf}Y_L^{fi}\log\Delta-\frac{1}{\Delta}\big(m_im_jz^2Y_L^{jf}Y_R^{fi}\big)\\ -\frac{1}{\Delta}\Big[m_fm_jzY_L^{jf}Y_L^{fi}+m_fm_izY_R^{jf}Y_R^{fi}+\big(q^2xy+m_f^2\big)Y_R^{jf}Y_L^{fi}\Big]\Big\},\tag{3.23}$$

where $\Delta\equiv zm_h^2-xzm_j^2-yzm_i^2+(x+y)m_f^2-xyq^2$ and $z\equiv1-x-y$. Here, $Q_q$ is the electric charge of quark $q$. $q^2$ denotes square of the moment exchange and takes the value



JHEP02(2019)007

of $-m_\mu^2$, which corresponds to the limit of an infinitely heavy nucleus. The coupling $g^q_{RV}$ can be obtained from $g^q_{LV}$ with the replacement $Y \to Y^\dagger$.

Using these Wilson coefficients, the rate of $\mu \to e$ conversion in a nuclei $N$ can be written as [69]

$$\Gamma(\mu N \to eN) = \left| -\frac{e}{16\pi^2} c_R D + \tilde{g}^{(p)}_{LS} S^{(p)} + \tilde{g}^{(n)}_{LS} S^{(n)} + \tilde{g}^{(p)}_{LV} V^{(p)} \right|^2 + \big(L \leftrightarrow R\big). \tag{3.24}$$

Here, $\tilde{g}^{(n,p)}_{L/RS,L/RV}$ denote the couplings to proton and neutron and can be evaluated from the quark-level ones

$$\begin{aligned} \tilde{g}^{(p)}_{LS,RS} &= \sum_q g^q_{LS,RS} \frac{m_p}{m_q} f^{(q,p)}\,, \qquad \tilde{g}^{(p)}_{LV,RV} = g^q_{LV,RV}/Q_q\,, \\ \tilde{g}^{(n)}_{LS,RS} &= \sum_q g^q_{LS,RS} \frac{m_n}{m_q} f^{(q,n)}\,, \end{aligned} \tag{3.25}$$

where the summation runs over all quark flavors $q \in \{u, d, s, c, b, t\}$, and the nucleon matrix elements $f^{(q,p)} \equiv \langle p | m_q \bar{q} q | p \rangle / m_p$ are numerically [70, 71]

$$\begin{aligned} &f^{(u,p)} = f^{(d,n)} = 0.024, \qquad f^{(c,p)} = f^{(b,p)} = f^{(t,p)} = \frac{2}{27}\left(1 - \sum_{q=u,d,s} f^{(q,p)}\right), \\ &f^{(d,p)} = f^{(u,n)} = 0.033, \qquad f^{(c,n)} = f^{(b,n)} = f^{(t,n)} = \frac{2}{27}\left(1 - \sum_{q=u,d,s} f^{(q,n)}\right), \\ &f^{(s,p)} = f^{(s,n)} = 0.25. \end{aligned} \tag{3.26}$$

The coefficients $D$, $V^{(p)}$, $S^{(p)}$, and $S^{(n)}$ denote overlap integrals of the muon, electron and nuclear wave function. For the Au and Al nuclei, their values read [69]

$$\big(D, V^{(p)}, S^{(p)}, S^{(n)}\big) = \begin{cases} 0.1890, 0.0974, 0.0614, 0.0918, & \text{for Au}, \\ 0.0362, 0.0161, 0.0155, 0.0167, & \text{for Al}, \end{cases} \tag{3.27}$$

in unit of $m_\mu^{5/2}$.

Finally, the branching ratio of $\mu \to e$ conversion are obtained

$$\mathcal{B}(\mu N \to eN) = \frac{\Gamma(\mu N \to eN)}{\Gamma_{\text{capt. } N}}, \tag{3.28}$$

where $\Gamma_{\text{capt. } N}$ denotes the muon capture rate, and numerically $\Gamma_{\text{capt. Au}} = 1.307 \times 10^7\,\text{s}^{-1}$ and $\Gamma_{\text{capt. Al}} = 7.054 \times 10^5\,\text{s}^{-1}$ [72].

## 4 Numerical analysis

In this section, we proceed to present our numerical analysis for the Higgs FCNC couplings in the general case and in the MFV framework presented in section 2.1 and section 2.2, respectively. Table 1 shows the relevant input parameters, and table 2 summarises the



JHEP02(2019)007

| Input | Value | Unit | Ref. |
|---|---|---|---|
| $\alpha_s^{(5)}(m_Z)$ | $0.1181 \pm 0.0011$ | | [74] |
| $m_t^{\rm P}$ | $173.1 \pm 0.9$ | GeV | [74] |
| $\lvert V_{cb}\rvert$ (semi-leptonic) | $41.00 \pm 0.33 \pm 0.74$ | $10^{-3}$ | [75] |
| $\lvert V_{ub}\rvert$ (semi-leptonic) | $3.98 \pm 0.08 \pm 0.22$ | $10^{-3}$ | [75] |
| $\lvert V_{us}\rvert f_+^{K\to\pi}(0)$ | $0.2165 \pm 0.0004$ | | [75] |
| $\gamma$ | $72.1^{+5.4}_{-5.8}$ | [°] | [75] |
| $f_+^{K\to\pi}(0)$ | $0.9681 \pm 0.0014 \pm 0.0022$ | | [75] |
| $\sin^2\theta_{12}$ | $0.307^{+0.013}_{-0.012}$ | | [76] |
| $\sin^2\theta_{23}$ | $0.538^{+0.033}_{-0.069}$ $(0.554^{+0.023}_{-0.033})$ | | [76] |
| $\sin^2\theta_{13}$ | $0.02206^{+0.00075}_{-0.00075}$ $(0.02227^{+0.00074}_{-0.00074})$ | | [76] |
| $\delta_{\rm CP}$ | $234^{+43}_{-31}$ $(278^{+26}_{-29})$ | [°] | [76] |
| $\Delta m^2_{21}$ | $7.40^{+0.21}_{-0.20}$ | $10^{-5}\,\text{eV}^2$ | [76] |
| $\Delta m^2_{3\ell}$ | $+2.494^{+0.033}_{-0.031}$ $(-2.465^{+0.032}_{-0.031})$ | $10^{-3}\,\text{eV}^2$ | [76] |
| $f_{B_s}$ | $228.4 \pm 3.7$ | MeV | [77] |
| $f_{B_d}$ | $192.0 \pm 4.3$ | MeV | [77] |
| $f_K$ | $155.7 \pm 0.7$ | MeV | [77] |
| $f_{B_s}\sqrt{\hat{B}_s}$ | $274 \pm 8$ | MeV | [77] |
| $f_{B_d}\sqrt{\hat{B}_d}$ | $225 \pm 9$ | MeV | [77] |
| $\hat{B}_K$ | $0.7625 \pm 0.0097$ | | [77] |
| $1/\Gamma_s^{\rm H}$ | $1.609 \pm 0.010$ | ps | [78] |
| $\Delta\Gamma_s/\Gamma_s$ | $0.128 \pm 0.009$ | | [78] |

**Table 1**. Input parameters used in the numerical analysis. The neutrino oscillation parameters (values in brackets) correspond to the normal (inverted) ordering of the light neutrinos' masses.

SM predictions and the current experimental data for various processes discussed in the previous sections.

To constrain the Higgs FCNC couplings, we impose the experimental constraints in the same way as in refs. [41, 73]; i.e., for each point in the parameter space, if the difference between the corresponding theoretical prediction and experimental data is less than $1.96\,\sigma$ ($1.65\,\sigma$) error bar, which is calculated by adding the theoretical and experimental errors in quadrature, this point is regarded as allowed at 95% CL (90% CL). Since the main theoretical uncertainties arise from hadronic input parameters, which are common to both the SM and the Higgs FCNC contributions, the relative theoretical uncertainty is assumed to be constant over the whole parameter space. As discussed in section 2.1, the numerical results in this section are valid only under the assumption that BSM effects to the low-energy flavor transitions are dominated by the effective operators listed in eq. (2.2).



JHEP02(2019)007

| OBSERVABLE | SM | EXP | Ref. |
|---|---|---|---|
| $\mathcal{B}(h \to e\mu)$ | - | $< 3.5 \times 10^{-4}$ | [11] |
| $\mathcal{B}(h \to e\tau)$ | - | $< 6.1 \times 10^{-3}$ | [12] |
| $\mathcal{B}(h \to \mu\tau)$ | - | $< 2.5 \times 10^{-3}$ | [12] |
| $\mathcal{B}(\mu \to e\gamma)$ | - | $< 4.2 \times 10^{-13}$ | [79] |
| $\mathcal{B}(\tau \to e\gamma)$ | - | $< 3.3 \times 10^{-8}$ | [74] |
| $\mathcal{B}(\tau \to \mu\gamma)$ | - | $< 4.4 \times 10^{-8}$ | [74] |
| $\mathcal{B}(\mu \to eee)$ | - | $< 1.0 \times 10^{-12}$ | [74] |
| $\mathcal{B}(\tau \to eee)$ | - | $< 2.7 \times 10^{-8}$ | [74] |
| $\mathcal{B}(\tau \to \mu\mu\mu)$ | - | $< 2.1 \times 10^{-8}$ | [74] |
| $\mathcal{B}(\mu\mathrm{Au} \to e\mathrm{Au})$ | - | $< 7.0 \times 10^{-13}$ | [80] |
| $\overline{\mathcal{B}}(B_s \to \mu^+\mu^-)[10^{-9}]$ | $3.43 \pm 0.19$ | $3.1 \pm 0.7$ | [78] |
| $\Delta m_d[\mathrm{ps}^{-1}]$ | $0.607^{+0.075}_{-0.075}$ | $0.5064 \pm 0.0019$ | [78] |
| $\Delta m_s[\mathrm{ps}^{-1}]$ | $19.196^{+1.377}_{-1.341}$ | $17.757 \pm 0.021$ | [78] |
| $\phi_s[\mathrm{rad}]$ | $-0.042^{+0.003}_{-0.003}$ | $-0.021 \pm 0.031$ | [78] |
| $\Delta m_K[10^{-3}\,\mathrm{ps}^{-1}]$ | $4.68 \pm 1.88$ | $5.293 \pm 0.009$ | [74] |
| $\lvert\varepsilon_K\rvert[10^{-3}]$ | $2.33^{+0.27}_{-0.29}$ | $2.228 \pm 0.011$ | [74] |

**Table 2**. SM predictions and experimental measurements for the observables used in the numerical analysis. Upper bounds for the Higgs LFV decays are values corresponding to 95% CL, while the other LFV processes 90% CL.

### 4.1 Analysis within general Higgs FCNC

In our previous paper [41], the Higgs LFV interactions in eq. (2.5) have already been studied in detail. Here, we focus on the couplings $Y^{e\mu}_{L,R}$ and $Y^{e\tau}_{L,R}$. These two couplings could induce $h \to e\mu$ and $h \to e\tau$ decay, respectively. The current Higgs data give the following bounds

$$\sqrt{|Y^{e\mu}_L|^2 + |Y^{e\mu}_R|^2} < 7.2 \times 10^{-4}\,, \qquad \text{and} \qquad \sqrt{|Y^{e\tau}_L|^2 + |Y^{e\tau}_R|^2} < 3.0 \times 10^{-3}\,, \tag{4.1}$$

at 95% CL. When obtaining these bounds, the contributions of $Y^{e\mu}_{L,R}$ and $Y^{e\tau}_{L,R}$ to the Higgs total width have been included.

The FCNC couplings $Y_{sb}$ and $\bar{Y}_{sb}$ are constrained by $B_s - \bar{B}_s$ mixing. In the case of real $Y_{sb}$ and $\bar{Y}_{sb}$, their allowed regions obtained from $\Delta m_s$ are shown in figure 1. There are two allowed regions. The one near the origin corresponds to the case where the Higgs FCNC effects are destructive with the SM contribution. In the other region, the Higgs-mediated FCNC interactions dominate over the SM contribution. Another bound on these two parameters comes from the $h \to sb$ decay. Although there is no upper limits on this process currently, we consider the bound $\mathcal{B}(h \to \text{new}) < 34\%$ at 95%CL, which is obtained from a global fit of the LHC run I data and applies to modifications of the decays into



JHEP02(2019)007

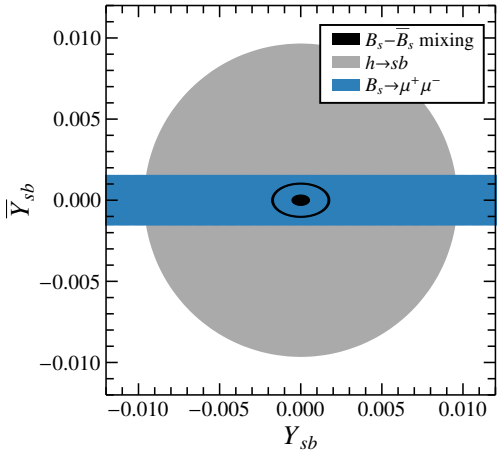


**Figure 1**. Allowed region of $(Y_{sb}, \bar{Y}_{sb})$ at 95% CL, assuming real $Y_{sb}$ and $\bar{Y}_{sb}$ couplings. The black region corresponds to the allowed parameter space by $B_s - \bar{B}_s$ mixing. The blue region is allowed by $\mathcal{B}(B_s \to \mu^+\mu^-)$ with the assumption $(Y_{\mu\mu}, \bar{Y}_{\mu\mu}) = (Y_{\mu\mu}^{\rm SM}, 0)$. In the dark region, $\Gamma(h \to sb) < 1.4\,\text{MeV}$.

SM particles that are not directly measured by the LHC [81]. However, this constraint is much weaker than the one from $B_s - \bar{B}_s$ mixing, as shown in figure 1. Furthermore, assuming a SM-like $h\mu\mu$ coupling, $\mathcal{B}(B_s \to \mu^+\mu^-)$ also provides a constraint on $\bar{Y}_{sb}$. Such constraint is comparable with the one from $B_s - \bar{B}_s$ mixing, as can be seen in figure 1. In the case of complex $Y_{sb}$ and $\bar{Y}_{sb}$, situation becomes quite different. Since the contributions of $Y_{sb}$ and $\bar{Y}_{sb}$ to $\Delta m_s$ can cancel out each other, $B_s - \bar{B}_s$ mixing can't provide upper limits on $|Y_{sb}|$ and $|\bar{Y}_{sb}|$. In this case, the upper limits are given by $\mathcal{B}(B_s \to \mu^+\mu^-)$ with the assumption of a SM-like $h\mu\mu$ coupling and are weaker than the ones in the case of real couplings. Finally, the combined constraints on the complex couplings $Y_{sb}$ and $\bar{Y}_{sb}$ result in the following prediction

$$\Gamma(h \to sb) < 0.17\,\text{MeV},$$

at 95% CL.

For the $B_s \to \ell_1\ell_2$ decays, using the analytical expressions in section 3, we can obtain the following numerical expression

$$\frac{\mathcal{B}(B_s \to \ell_1\ell_2)}{\mathcal{B}(h \to \ell_1\ell_2)} \approx 2.1|\bar{Y}_{sb}|^2\,, \tag{4.2}$$

where the SM Higgs total width $\Gamma_h^{\rm SM} \approx 4.07\,\text{MeV}$ [82] is assumed. In the case of complex Yukawa couplings, the combined bounds on $Y_{sb}$ and $\bar{Y}_{sb}$ discussed above and the LHC bounds on $h \to \ell_i\ell_j$ result in following upper limits

$$\mathcal{B}(B_s \to e\mu) < 2.1 \times 10^{-9}\,, \quad \mathcal{B}(B_s \to e\tau) < 3.7 \times 10^{-8}\,, \quad \mathcal{B}(B_s \to \mu\tau) < 1.5 \times 10^{-8}\,,$$

at 95% CL. For the branching ratio of $B_s \to e\mu$ decay, our predicted upper limit is three times lower than the current LHCb bound $\mathcal{B}(B_s \to e\mu) < 6.3 \times 10^{-9}$ [10].



JHEP02(2019)007

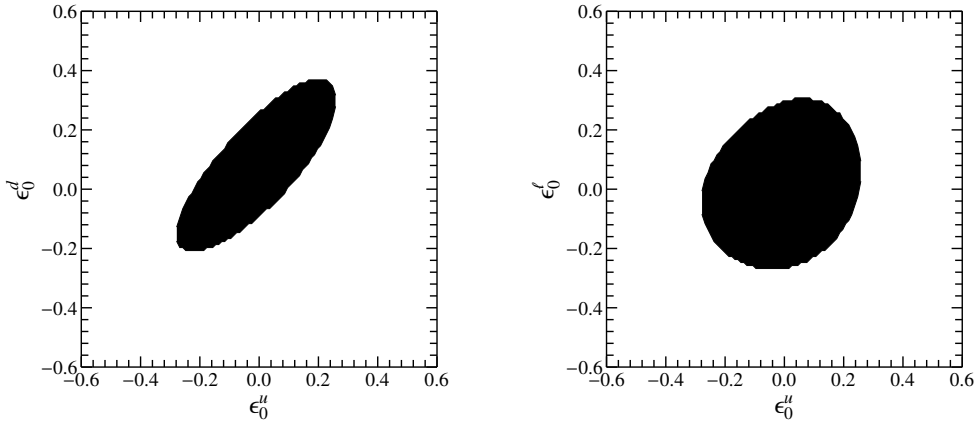


**Figure 2**. Allowed region of $(\epsilon_0^u,\, \epsilon_0^d,\, \epsilon_0^\ell)$ by the LHC Higgs data at 90% CL, plotted in the $(\epsilon_0^u,\, \epsilon_0^d)$ (left) and $(\epsilon_0^u,\, \epsilon_0^\ell)$ (right) plane.

The Higgs FCNC couplings can also affect the LFV processes in the lepton sector, such as the $\mu \to e\gamma$ decay. However, their dominated contributions arise at loop level and involve several Yukawa couplings. These processes can't provide model-independent bounds on one or two particular Yukawa couplings except assuming some special hierarchy among the Higgs FCNC couplings $Y_{L,R}^{i,j}$, as in ref. [5].

### 4.2 Analysis in the MFV framework

The Higgs FCNC couplings in the MFV framework have been discussed in detail in section 2.2. In the following numerical analysis, without loss of generality, we take the NP scale $\Lambda = v$, such that $\hat{\epsilon}_{0,1,2}^{u,d,\ell} = \epsilon_{0,1,2}^{u,d,\ell}$,[1] and the right-handed neutrinos' mass $\mathcal{M} = 10^{15}\,\text{GeV}$. For the MFV in the lepton sector, we consider the simplest possibility that the orthogonal matrix $O$ in eq. (2.19) is real. Since mass ordering of light neutrinos is not yet established, both the normal ordering (NO), where $m_1 < m_2 < m_3$, and the inverted ordering (IO), where $m_3 < m_1 < m_2$, are included in our analysis. In the NO (IO) case, we take $m_{1(3)} = 0$. Finally, the Higgs Yukawa couplings in the MFV framework are determined by the following 6 real parameters

$$\left(\epsilon_0^u,\ \epsilon_0^d,\ \epsilon_1^d,\ \epsilon_0^\ell,\ \epsilon_1^\ell,\ \epsilon_2^\ell\right), \tag{4.3}$$

which correspond to the up-type quark, down-type quark and lepton sectors, respectively. In the following, the constraints on these parameters will be discussed in detail.

The parameters $(\epsilon_0^u,\, \epsilon_0^d,\, \epsilon_0^\ell)$ control the Higgs flavor-conserving couplings to up-type quarks, down-type quarks and leptons, respectively. They are constrained by the Higgs production and decays processes at the LHC. We perform a global fit for these three parameters with the `Lilith` package [83], which is used to take into account the Higgs data measured by LHC Run I [81] and Tevatron [84]. Although the flavor-changing parameters $\epsilon_1^d$ and $\epsilon_{1,2}^\ell$ can also affect the Higgs signal strengths, they are strongly bounded by

[1] In other words, the parameters $\epsilon_{0,1,2}^{u,d,\ell}$ in this subsection are actually $\hat{\epsilon}_{0,1,2}^{u,d,\ell}$.



JHEP02(2019)007

other processes, as discussed in the following. Therefore, their contributions can be safely neglected in the global fit. The allowed regions of $(\epsilon_0^u,\, \epsilon_0^d,\, \epsilon_0^\ell)$ at 90% CL are shown in figure 2. Our global fit shows that $\mathcal{O}(30\%)$ deviations from the SM values are allowed for the flavor-conserving couplings in the MFV framework.

The flavor-changing couplings for down-type quarks are determined by the parameter $\epsilon_1^d$. Constraints on this coupling come from $B_s - \bar{B}_s$, $B_d - \bar{B}_d$ and $K^0 - \bar{K}^0$ mixing. Since hadronic uncertainties in $K^0 - \bar{K}^0$ mixing are relatively large [85, 86], we adopt the conservative treatment in ref. [86]; i.e., the Higgs FCNC effects to $\Delta m_K$ are allowed within 50% range of $\Delta m_K^{\rm exp}$, and $|\epsilon_K|$ is allowed to vary within a 20% symmetric range. Since the current experimental data of the $B$ and $K$ mixing are in good agreement with the SM prediction, we obtain the strong bound on the MFV parameter

$$|\epsilon_1^d| < 0.59, \tag{4.4}$$

at 95% CL. This bound is dominated by $\Delta m_s$ in $B_s - \bar{B}_s$ mixing. Since the Yukawa couplings $Y_{L,R}^{sd}$ in the MFV framework are suppressed by $s$ or $d$ quark mass as in eq. (2.16), $K^0 - \bar{K}^0$ mixing can't provide strong constraint. Using this bound, the predicted upper limits for various Higgs FCNC decays are obtained

$$\begin{aligned}
\Gamma(h \to sd) &< 7.4 \times 10^{-11}\ \text{MeV}, \\
\Gamma(h \to sb) &< 2.0 \times 10^{-3}\ \ \text{MeV}, \\
\Gamma(h \to db) &< 9.4 \times 10^{-5}\ \ \text{MeV},
\end{aligned} \tag{4.5}$$

at 95% CL. These channels suffer from a huge QCD background which makes measurement of these decays very challenging at the LHC, and even at the ILC. At a centre-of-mass energy 500 GeV with an integrated luminosity of 4000 fb$^{-1}$, ILC can provide a discovery sensitivity of 0.5% for $\mathcal{B}(h \to bj)$, with $j$ representing a light quark [87], which is still about one order of magnitude larger than these upper limits listed above.

The parameters $(\epsilon_1^\ell,\, \epsilon_2^\ell)$ control the flavor-changing couplings for charged leptons. They should be bounded by the LFV processes. However, as discussed in section 3, the quark Yukawa couplings also appear in some leptonic processes, e.g., top quark Yukawa couplings are involved in the two-loop diagrams of $\mu \to e\gamma$ and all the quark Yukawa couplings affect $\mu \to e$ conversion in nuclei at the tree level. Generally, all relevant parameters in the LFV processes are $(\epsilon_0^u,\, \epsilon_0^d,\, \epsilon_0^\ell,\, \epsilon_1^\ell,\, \epsilon_2^\ell)$. We don't include the MFV parameter $\epsilon_1^d$, since its effect is highly suppressed in the LFV processes. When deriving the bounds on these parameters and studying their effects, it's useful to separate from the effects of the quark Yukawa couplings. Therefore, we consider the following two scenarios in the discussion of the LFV processes.

$$\begin{aligned}
&\text{Scenario I}: -0.5 < \epsilon_{0,1,2}^\ell < +0.5, \qquad \text{Scenario II}: -1.0 < \epsilon_{0,1,2}^\ell < +1.0, \\
&\epsilon_0^u = \epsilon_0^d = 0, \qquad\qquad -1.0 < \epsilon_0^{u,d} < +1.0,
\end{aligned} \tag{4.6}$$

Scenario I corresponds to the case that the flavor-conserving quark Yukawa couplings are the SM-like, and Scenario II the most general case.



JHEP02(2019)007

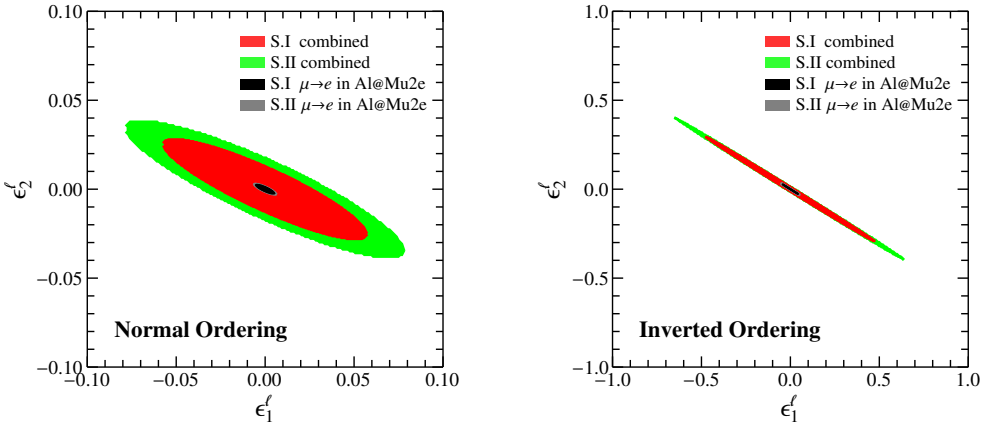


**Figure 3**. Combined constraints on $(\epsilon_0^u, \epsilon_0^d, \epsilon_0^\ell, \epsilon_1^\ell, \epsilon_2^\ell)$ at 90% CL, plotted in the $(\epsilon_1^\ell, \epsilon_2^\ell)$ plane, in the NO (Left) and IO (Right) cases, which are dominated by the $\mu \to e\gamma$ decay. The red and green regions are the allowed parameter space in Scenario I and II, respectively. The tiny black and dark regions indicate the future sensitivity to the $\mu \to e$ conversion in Al at the Mu2e experiment.

To constrain the MFV parameters, we consider various LFV processes including $h \to \ell_i\ell_j$, $\ell_i \to \ell_j\ell_k\bar{\ell}_l$, $\ell_i \to \ell_j\gamma$, $\mu \to e$ conversion in nuclei, leptonic EDM, and anomalous magnetic moment. The previously obtained bounds on $(\epsilon_0^u, \epsilon_0^d, \epsilon_0^\ell)$ from the Higgs data have been also included. After combining all these constraints, the allowed parameter space of $(\epsilon_0^u, \epsilon_0^d, \epsilon_0^\ell, \epsilon_1^\ell, \epsilon_2^\ell)$ are obtained for scenario I and II in the NO and IO cases, which are plotted in the $(\epsilon_1^\ell, \epsilon_2^\ell)$ plane in figure 3. All the correlations are showing in figure 6 in appendix A, from which one can see the correlations between the flavor-conserving couplings $(\epsilon_0^u, \epsilon_0^d, \epsilon_0^\ell)$ and the flavor-changing couplings $(\epsilon_1^\ell, \epsilon_2^\ell)$ are weak. It is found that the most strong constraints on the MFV parameters come from the branching ratio of $\mu \to e\gamma$ decay. Our detailed numerical analysis shows that the $\mu \to e\gamma$ decay in the allowed parameter space is dominated by the two-loop contribution $c_R^{2-\text{loop}}$ in eq. (3.19), which is proportional to the couplings $Y_R^{e\mu}$ and $Y_L^{tt}$. Due to the values of the PMNS matrix in the IO case, the contributions from $\epsilon_1^\ell$ and $\epsilon_2^\ell$ can strongly cancel out each other in the Yukawa couplings $Y_R^{e\mu}$. It makes the allowed ranges of $\epsilon_1^\ell$ and $\epsilon_2^\ell$ in the IO case are much wider than the one in the NO case but have larger fine-tuning.

For comparison, the bounds from $\mu \to e$ conversion in Au are shown in figure 4, which are much weaker than ones from the $\mu \to e\gamma$ decay. In the future Mu2e experiment, the sensitivity for the branching ratio of $\mu \to e$ conversion is expected to be improved by 4 orders of magnitude compared to the current SINDRUM II bound, which corresponds to $7 \times 10^{-17}$ in Al at 90% CL [16]. The allowed parameter space corresponding to the future sensitivity at the Mu2e experiment are shown in figure 3. It can be seen that the expected bounds at the Mu2e experiment are much more stringent than the ones obtained from the current measurements on $\mu \to e\gamma$ decay. In the near future, with three-year run, the MEG II experiment can reach a sensitivity of $6 \times 10^{-14}$ at 90% CL for $\mathcal{B}(\mu \to e\gamma)$ [88]. However, the corresponding bounds on the MFV parameters are much weaker than the ones expected at the Mu2e experiment.



JHEP02(2019)007

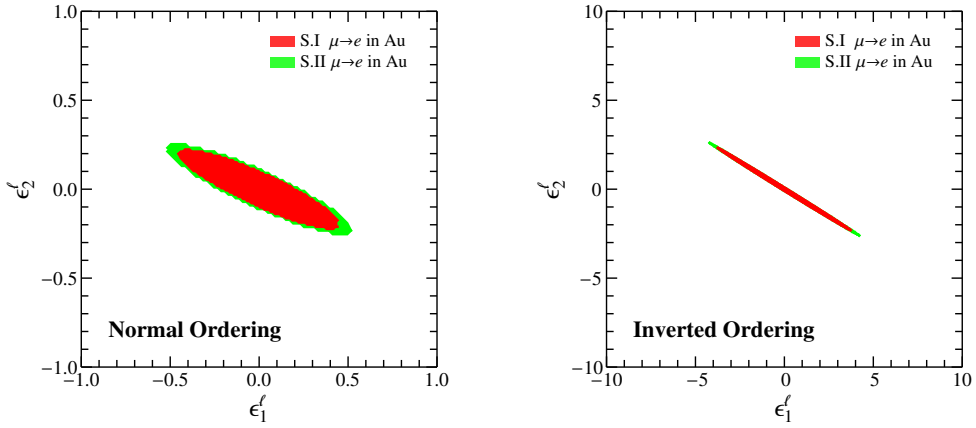


**Figure 4**. The same as figure 3, but only under the constraint of $\mu \to e$ conversion in Au.

| | | $\Gamma(h \to e\mu)$ | $\Gamma(h \to e\tau)$ | $\Gamma(h \to \mu\tau)$ | $\mathcal{B}(B_s \to e\mu)$ | $\mathcal{B}(B_s \to e\tau)$ | $\mathcal{B}(B_s \to \mu\tau)$ |
|---|---|---|---|---|---|---|---|
| NO | S.I | $1.2\times10^{-8}$ | $1.3\times10^{-5}$ | $9.0\times10^{-5}$ | $2.4\times10^{-16}$ | $2.6\times10^{-13}$ | $1.8\times10^{-12}$ |
| NO | S.II | $2.2\times10^{-8}$ | $2.4\times10^{-5}$ | $1.7\times10^{-4}$ | $4.6\times10^{-16}$ | $5.0\times10^{-13}$ | $3.5\times10^{-12}$ |
| IO | S.I | $1.2\times10^{-8}$ | $4.7\times10^{-6}$ | $7.1\times10^{-5}$ | $2.4\times10^{-16}$ | $9.6\times10^{-14}$ | $1.4\times10^{-12}$ |
| IO | S.II | $2.2\times10^{-8}$ | $8.7\times10^{-6}$ | $1.3\times10^{-4}$ | $4.5\times10^{-16}$ | $1.8\times10^{-13}$ | $2.6\times10^{-12}$ |

**Table 3**. Upper bounds on $\Gamma(h \to \ell_i\ell_j)$ [MeV] and $\mathcal{B}(B_s \to \ell_i\ell_j)$ at 90%CL.

Since the experimental sensitivity to the LFV processes $\mu \to e\gamma$ and $\mu \to e$ conversion in nuclei will be greatly improved in the near future, we show the correlations between $\mathcal{B}(\mu \to e\gamma)$ and $\mathcal{B}(\mu\,\mathrm{Al} \to e\,\mathrm{Al})$ in figure 5, which are obtained in the allowed parameter space corresponding to figure 3. It can be seen that, the correlations in the NO and IO cases are almost the same. To understand this, we should notice that the Higgs FCNC effects on these two processes are dominated by the contributions of $c_R^{2-\mathrm{loop}}$ and $g_{LS}^q$ in the allowed parameter space in both the NO and IO cases. In the scenario I, from their definitions in eq. (3.19) and (3.22), they are proportional to the Yukawa coupling $Y_R^{e\mu}$, which makes the branching ratios of both the two processes are proportional to $|Y_R^{e\mu}|^2$. Therefore, although $Y_R^{e\mu}$ depends on $(\epsilon_1^\ell,\, \epsilon_2^\ell)$ differently in the NO and IO cases, the correlation between $\mathcal{B}(\mu\,\mathrm{Al} \to e\,\mathrm{Al})$ and $\mathcal{B}(\mu \to e\gamma)$ is very strong and does no depend on the ordering of the light neutrinos' masses, as shown by the thin red regions in figure 5. In the scenario II, the contributions $c_R^{2-\mathrm{loop}}$ and $g_{LS}^q$ are also proportional to $Y_L^{tt}$ and $Y_R^{qq}$, respectively. In the MFV framework, the flavor-conserving couplings $Y_L^{tt}$ and $Y_R^{qq}$ mainly depend on the parameters $(\epsilon_0^u,\, \epsilon_0^d)$ and their dependence are the same between in the NO and IO cases. These flavor-conserving couplings make the correlation between $\mathcal{B}(\mu\,\mathrm{Al} \to e\,\mathrm{Al})$ and $\mathcal{B}(\mu \to e\gamma)$ much weaker than the one in the scenario I in both the NO and IO cases, as shown by the wide green regions in figure 5. Considering that the bounds on the flavor-conserving couplings will be largely improved by the future LHC data, the correlation in the scenario II is expected to become much stronger and approach the one in the scenario I.



JHEP02(2019)007

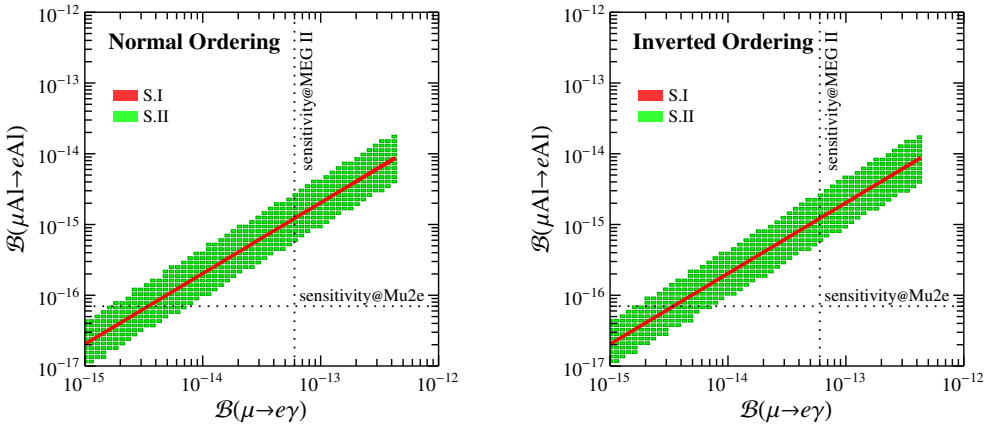


**Figure 5**. Correlation between $\mathcal{B}(\mu \to e\gamma)$ and $\mathcal{B}(\mu\text{Au} \to e\text{Au})$, in the NO (left) and IO (right) cases. The red and black region denotes the S.I and S.II, respectively.

For the anomalous magnetic moment $a_\mu$, current data show about $3\sigma$ deviation from the SM prediction [74, 89]. In the MFV framework, explanation for this anomaly needs large LFV parameters $\epsilon_1^\ell$ and $\epsilon_2^\ell$, which is ruled out by the $\mu \to e\gamma$ decay.

Using the combined bounds obtained in the previous sections, the upper limits on various LFV $B_s$ and Higgs decays are obtained for the scenario I and II and in the NO and IO cases, which are shown in table 3. For the $h \to \mu\tau$ decay, the upper limits in the MFV are about two orders of magnitude lower than the current LHC bounds, which make searches for this channel challenging at the LHC. For the other LFV decays, since the upper bounds on their branching ratios are lower than the current LHC bounds by several orders of magnitude, they are very difficult to be measured at the LHC. For the $B_s \to \mu^+\mu^-$ decay in both the NO and IO cases, it is found that its branching ratio can't deviate from the SM prediction by more than 1%.

## 5 Conclusions

Motivated by the recent LHC searches for the LFV decays $B_s \to \ell_i\ell_j$ and $h \to \ell_i\ell_j$, we study the tree-level Higgs FCNC interactions in the EFT approach. With and without the MFV hypothesis, we investigate the Higgs FCNC effects on the $B_s - \bar{B}_s$, $B_d - \bar{B}_d$ and $K^0 - \bar{K}^0$ mixing, the lepton FCNC processes $\ell_i \to \ell_j\gamma$, $\ell_i \to \ell_j\ell_k\bar{\ell}_l$, $\mu \to e$ conversion in nuclei, the LHC Higgs data, and etc, and derive the bounds on the Higgs FCNC couplings.

In the general case, the two LFV decays $B_s \to \ell_1\ell_2$ and $h \to \ell_1\ell_2$ are related to each other by the following expression

$$\frac{\mathcal{B}(B_s \to \ell_1\ell_2)}{\mathcal{B}(h \to \ell_1\ell_2)} \approx 2.1|\bar{Y}_{sb}|^2,$$

assuming the SM Higgs total width. After deriving the bounds on $\bar{Y}_{sb}$ from $B_s - \bar{B}_s$ mixing and $B_s \to \mu^+\mu^-$, predictions on various Higgs and $B_s$ FCNC decays are obtained, such as

$$\mathcal{B}(B_s \to e\mu) < 2.1 \times 10^{-9}, \qquad \mathcal{B}(h \to sb) < 4.1 \times 10^{-2},$$

at 95% CL, where the SM Higgs total width is assumed.



JHEP02(2019)007

In the MFV hypothesis, strong constraints on the free parameters ($\epsilon_0^u$, $\epsilon_0^d$, $\epsilon_1^d$, $\epsilon_0^\ell$, $\epsilon_1^\ell$, $\epsilon_2^\ell$) are derived. We find that the bounds on ($\epsilon_0^u$, $\epsilon_0^d$, $\epsilon_0^\ell$) are dominated by the LHC Higgs data, $\epsilon_1^d$ the $B_s - \bar{B}_s$ mixing, and ($\epsilon_1^\ell$, $\epsilon_2^\ell$) the $\mu \to e\gamma$ decay. Using these constraints, we obtain upper limits on various FCNC processes, such as

$$\mathcal{B}(h \to sb) < 4.9 \times 10^{-4},$$

at 95% CL, and for the normal (inverted) ordering of the light neutrinos' masses,

$$\mathcal{B}(h \to \mu\tau) < 4.2\,(3.2) \times 10^{-5}, \qquad \mathcal{B}(B_s \to e\mu) < 4.6\,(4.5) \times 10^{-16},$$

at 90% CL, where the SM Higgs total width is assumed. For the $B_s \to \mu^+\mu^-$ decay, its branching ratio can't deviate from the SM prediction by more than 1%. For the various $B_s \to \ell_1\ell_2$ and $h \to \ell_1\ell_2$ decays, since the upper limits of their branching ratios are much lower than the current LHC bounds, searches for these LFV processes are very challenging at the LHC. However, with the improved measurements at the future MEG II and Mu2e experiments, searches for the LFV Higgs couplings in the $\mu \to e\gamma$ decay and $\mu \to e$ conversion in Al are very promising. In the MFV, the branching ratios of these two processes are strongly correlated to each other. Our bounds and correlations for the various processes can be used to obtain valuable information about the Higgs FCNC couplings from future measurements at the LHC and the low-energy experiments.


## Acknowledgments

This work was supported in part by the MOST (Grant No. MOST 106-2112-M-002-003-MY3 ), and in part by Key Laboratory for Particle Physics, Astrophysics and Cosmology, Ministry of Education, and Shanghai Key Laboratory for Particle Physics and Cosmology (Grant No. 15DZ2272100), and in part by the NSFC (Grant Nos. 11575111 and 11735010). XY thanks Chen Zhang for useful discussions, and CCNU for its hospitality, where this work was partly conducted. This work was supported in part by the NSFC (Grant Nos. 11575111 and 11735010), and in part by Key Laboratory for Particle Physics, Astrophysics and Cosmology, Ministry of Education, and Shanghai Key Laboratory for Particle Physics and Cosmology (Grant No. 15DZ2272100), and also supported by the MOST (Grant No. MOST 106-2112-M-002-003-MY3).


## A Allowed parameter space in scenario II

In section 4, allowed parameter space of $(\epsilon_0^u, \epsilon_0^d, \epsilon_0^\ell, \epsilon_1^\ell, \epsilon_2^\ell)$ in scenario II are derived. The results in $(\epsilon_0^u, \epsilon_0^d)$ and $(\epsilon_0^u, \epsilon_0^\ell)$, and $(\epsilon_1^\ell, \epsilon_2^\ell)$ plane have been shown in figure 2 and figure 3, respectively. Here, we show the results in the other planes in figure 6.



JHEP02(2019)007

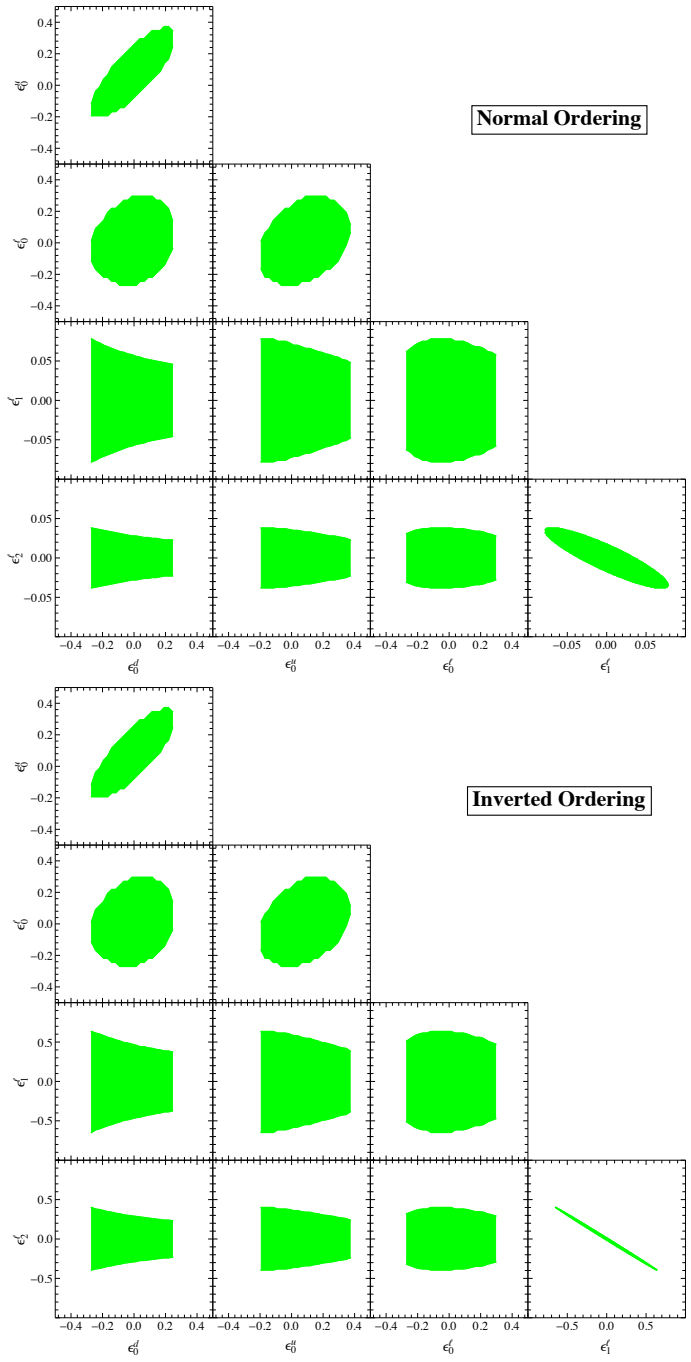


**Figure 6**. Combined constraints on $(\epsilon_0^u, \epsilon_0^d, \epsilon_0^\ell, \epsilon_1^\ell, \epsilon_2^\ell)$ at 90% CL in scenario II. Allowed regions in the NO and IO cases are shown in the upper and lower figures, respectively.





JHEP02(2019)007

## References


[1] ATLAS collaboration, *Observation of a new particle in the search for the Standard Model Higgs boson with the ATLAS detector at the LHC*, *Phys. Lett.* **B 716** (2012) 1 [arXiv:1207.7214] [INSPIRE].

[2] CMS collaboration, *Observation of a new boson at a mass of 125 GeV with the CMS experiment at the LHC*, *Phys. Lett.* **B 716** (2012) 30 [arXiv:1207.7235] [INSPIRE].

[3] C. Csáki, C. Grojean and J. Terning, *Alternatives to an elementary Higgs*, *Rev. Mod. Phys.* **88** (2016) 045001 [arXiv:1512.00468] [INSPIRE].

[4] C. Mariotti and G. Passarino, *Higgs boson couplings: measurements and theoretical interpretation*, *Int. J. Mod. Phys.* **A 32** (2017) 1730003 [arXiv:1612.00269] [INSPIRE].

[5] R. Harnik, J. Kopp and J. Zupan, *Flavor violating Higgs decays*, *JHEP* **03** (2013) 026 [arXiv:1209.1397] [INSPIRE].

[6] X.-G. He and G. Valencia, *The $Z \to b\bar{b}$ decay asymmetry and left-right models*, *Phys. Rev.* **D 66** (2002) 013004 [*Erratum ibid.* **D 66** (2002) 079901] [hep-ph/0203036] [INSPIRE].

[7] C.-W. Chiang, N.G. Deshpande, X.-G. He and J. Jiang, *The family $\mathrm{SU}(2)_l \times \mathrm{SU}(2)_h \times \mathrm{U}(1)$ model*, *Phys. Rev.* **D 81** (2010) 015006 [arXiv:0911.1480] [INSPIRE].

[8] G.C. Branco, P.M. Ferreira, L. Lavoura, M.N. Rebelo, M. Sher and J.P. Silva, *Theory and phenomenology of two-Higgs-doublet models*, *Phys. Rept.* **516** (2012) 1 [arXiv:1106.0034] [INSPIRE].

[9] A. Crivellin, A. Kokulu and C. Greub, *Flavor-phenomenology of two-Higgs-doublet models with generic Yukawa structure*, *Phys. Rev.* **D 87** (2013) 094031 [arXiv:1303.5877] [INSPIRE].

[10] LHCb collaboration, *Search for the lepton-flavour violating decays $B^0_{(s)} \to e^{\pm}\mu^{\mp}$*, *JHEP* **03** (2018) 078 [arXiv:1710.04111] [INSPIRE].

[11] CMS collaboration, *Search for lepton flavour violating decays of the Higgs boson to $e\tau$ and $e\mu$ in proton-proton collisions at $\sqrt{s} = 8$ TeV*, *Phys. Lett.* **B 763** (2016) 472 [arXiv:1607.03561] [INSPIRE].

[12] CMS collaboration, *Search for lepton flavour violating decays of the Higgs boson to $\mu\tau$ and $e\tau$ in proton-proton collisions at $\sqrt{s} = 13$ TeV*, *JHEP* **06** (2018) 001 [arXiv:1712.07173] [INSPIRE].

[13] CMS collaboration, *Search for lepton-flavour-violating decays of the Higgs boson*, *Phys. Lett.* **B 749** (2015) 337 [arXiv:1502.07400] [INSPIRE].

[14] G. Blankenburg, J. Ellis and G. Isidori, *Flavour-changing decays of a 125 GeV Higgs-like particle*, *Phys. Lett.* **B 712** (2012) 386 [arXiv:1202.5704] [INSPIRE].

[15] X.-G. He, J. Tandean and Y.-J. Zheng, *Higgs decay $h \to \mu\tau$ with minimal flavor violation*, *JHEP* **09** (2015) 093 [arXiv:1507.02673] [INSPIRE].

[16] MU2E collaboration, *Expression of interest for evolution of the Mu2e experiment*, arXiv:1802.02599 [INSPIRE].

[17] LHCb collaboration, *Test of lepton universality using $B^+ \to K^+\ell^+\ell^-$ decays*, *Phys. Rev. Lett.* **113** (2014) 151601 [arXiv:1406.6482] [INSPIRE].




JHEP02(2019)007

[18] LHCb collaboration, *Test of lepton universality with $B^0 \to K^{*0}\ell^+\ell^-$ decays*, *JHEP* **08** (2017) 055 [arXiv:1705.05802] [INSPIRE].

[19] Heavy Flavor Averaging Group (HFAG) collaboration, *Averages of b-hadron, c-hadron and $\tau$-lepton properties as of summer* 2014, arXiv:1412.7515 [INSPIRE].

[20] S. Fajfer, J.F. Kamenik, I. Nisandzic and J. Zupan, *Implications of lepton flavor universality violations in B decays*, *Phys. Rev. Lett.* **109** (2012) 161801 [arXiv:1206.1872] [INSPIRE].

[21] A. Crivellin, C. Greub and A. Kokulu, *Explaining $B \to D\tau\nu$, $B \to D^*\tau\nu$ and $B \to \tau\nu$ in a 2HDM of type-III*, *Phys. Rev.* **D 86** (2012) 054014 [arXiv:1206.2634] [INSPIRE].

[22] K.-F. Chen, W.-S. Hou, C. Kao and M. Kohda, *When the Higgs meets the top: search for $t \to ch^0$ at the LHC*, *Phys. Lett.* **B 725** (2013) 378 [arXiv:1304.8037] [INSPIRE].

[23] C.S. Kim, Y.W. Yoon and X.-B. Yuan, *Exploring top quark FCNC within 2HDM type-III in association with flavor physics*, *JHEP* **12** (2015) 038 [arXiv:1509.00491] [INSPIRE].

[24] A. Crivellin, J. Heeck and P. Stoffer, *A perturbed lepton-specific two-Higgs-doublet model facing experimental hints for physics beyond the Standard Model*, *Phys. Rev. Lett.* **116** (2016) 081801 [arXiv:1507.07567] [INSPIRE].

[25] R.S. Chivukula and H. Georgi, *Composite technicolor Standard Model*, *Phys. Lett.* **B 188** (1987) 99 [INSPIRE].

[26] A.J. Buras, P. Gambino, M. Gorbahn, S. Jager and L. Silvestrini, *Universal unitarity triangle and physics beyond the Standard Model*, *Phys. Lett.* **B 500** (2001) 161 [hep-ph/0007085] [INSPIRE].

[27] G. D'Ambrosio, G.F. Giudice, G. Isidori and A. Strumia, *Minimal flavor violation: an effective field theory approach*, *Nucl. Phys.* **B 645** (2002) 155 [hep-ph/0207036] [INSPIRE].

[28] B. Grzadkowski, M. Iskrzynski, M. Misiak and J. Rosiek, *Dimension-six terms in the Standard Model Lagrangian*, *JHEP* **10** (2010) 085 [arXiv:1008.4884] [INSPIRE].

[29] A.L. Fitzpatrick, G. Perez and L. Randall, *Flavor anarchy in a Randall-Sundrum model with 5D minimal flavor violation and a low Kaluza-Klein scale*, *Phys. Rev. Lett.* **100** (2008) 171604 [arXiv:0710.1869] [INSPIRE].

[30] A. Azatov, M. Toharia and L. Zhu, *Higgs mediated FCNC's in warped extra dimensions*, *Phys. Rev.* **D 80** (2009) 035016 [arXiv:0906.1990] [INSPIRE].

[31] M. Redi and A. Weiler, *Flavor and CP invariant composite Higgs models*, *JHEP* **11** (2011) 108 [arXiv:1106.6357] [INSPIRE].

[32] B. Bellazzini, C. Csáki and J. Serra, *Composite Higgses*, *Eur. Phys. J.* **C 74** (2014) 2766 [arXiv:1401.2457] [INSPIRE].

[33] F. del Aguila, M. Pérez-Victoria and J. Santiago, *Observable contributions of new exotic quarks to quark mixing*, *JHEP* **09** (2000) 011 [hep-ph/0007316] [INSPIRE].

[34] H. Bélusca-Maïto, A. Falkowski, D. Fontes, J.C. Romão and J.P. Silva, *Higgs EFT for 2HDM and beyond*, *Eur. Phys. J.* **C 77** (2017) 176 [arXiv:1611.01112] [INSPIRE].

[35] S. Davidson, *$\mu \to e\gamma$ in the 2HDM: an exercise in EFT*, *Eur. Phys. J.* **C 76** (2016) 258 [arXiv:1601.01949] [INSPIRE].

[36] S. Dawson and C.W. Murphy, *Standard Model EFT and extended scalar sectors*, *Phys. Rev.* **D 96** (2017) 015041 [arXiv:1704.07851] [INSPIRE].

JHEP02(2019)007

[37] K. Agashe and R. Contino, *Composite Higgs-mediated FCNC*, *Phys. Rev.* **D 80** (2009) 075016 [arXiv:0906.1542] [INSPIRE].

[38] J. Aebischer, A. Crivellin, M. Fael and C. Greub, *Matching of gauge invariant dimension-six operators for $b \to s$ and $b \to c$ transitions*, *JHEP* **05** (2016) 037 [arXiv:1512.02830] [INSPIRE].

[39] M. Raidal and A. Santamaria, *Muon electron conversion in nuclei versus $\mu \to e\gamma$: an effective field theory point of view*, *Phys. Lett.* **B 421** (1998) 250 [hep-ph/9710389] [INSPIRE].

[40] A. Crivellin, S. Davidson, G.M. Pruna and A. Signer, *Renormalisation-group improved analysis of $\mu \to e$ processes in a systematic effective-field-theory approach*, *JHEP* **05** (2017) 117 [arXiv:1702.03020] [INSPIRE].

[41] C.-W. Chiang, X.-G. He, F. Ye and X.-B. Yuan, *Constraints and implications on Higgs FCNC couplings from precision measurement of $B_s \to \mu^+\mu^-$ decay*, *Phys. Rev.* **D 96** (2017) 035032 [arXiv:1703.06289] [INSPIRE].

[42] G. Colangelo, E. Nikolidakis and C. Smith, *Supersymmetric models with minimal flavour violation and their running*, *Eur. Phys. J.* **C 59** (2009) 75 [arXiv:0807.0801] [INSPIRE].

[43] L. Mercolli and C. Smith, *EDM constraints on flavored CP-violating phases*, *Nucl. Phys.* **B 817** (2009) 1 [arXiv:0902.1949] [INSPIRE].

[44] X.-G. He, C.-J. Lee, S.-F. Li and J. Tandean, *Fermion EDMs with minimal flavor violation*, *JHEP* **08** (2014) 019 [arXiv:1404.4436] [INSPIRE].

[45] X.-G. He, C.-J. Lee, S.-F. Li and J. Tandean, *Large electron electric dipole moment in minimal flavor violation framework with Majorana neutrinos*, *Phys. Rev.* **D 89** (2014) 091901 [arXiv:1401.2615] [INSPIRE].

[46] X.-G. He, C.-J. Lee, J. Tandean and Y.-J. Zheng, *Seesaw models with minimal flavor violation*, *Phys. Rev.* **D 91** (2015) 076008 [arXiv:1411.6612] [INSPIRE].

[47] C.-W. Chiang, X.-G. He, J. Tandean and X.-B. Yuan, *$R_{K^{(*)}}$ and related $b \to s\ell\bar{\ell}$ anomalies in minimal flavor violation framework with $Z'$ boson*, *Phys. Rev.* **D 96** (2017) 115022 [arXiv:1706.02696] [INSPIRE].

[48] V. Cirigliano, B. Grinstein, G. Isidori and M.B. Wise, *Minimal flavor violation in the lepton sector*, *Nucl. Phys.* **B 728** (2005) 121 [hep-ph/0507001] [INSPIRE].

[49] V. Cirigliano and B. Grinstein, *Phenomenology of minimal lepton flavor violation*, *Nucl. Phys.* **B 752** (2006) 18 [hep-ph/0601111] [INSPIRE].

[50] R. Alonso, G. Isidori, L. Merlo, L.A. Muñoz and E. Nardi, *Minimal flavour violation extensions of the seesaw*, *JHEP* **06** (2011) 037 [arXiv:1103.5461] [INSPIRE].

[51] D.N. Dinh, L. Merlo, S.T. Petcov and R. Vega-Álvarez, *Revisiting minimal lepton flavour violation in the light of leptonic CP-violation*, *JHEP* **07** (2017) 089 [arXiv:1705.09284] [INSPIRE].

[52] J.A. Casas and A. Ibarra, *Oscillating neutrinos and $\mu \to e, \gamma$*, *Nucl. Phys.* **B 618** (2001) 171 [hep-ph/0103065] [INSPIRE].

[53] A.J. Buras, S. Jager and J. Urban, *Master formulae for $\Delta F = 2$ NLO QCD factors in the Standard Model and beyond*, *Nucl. Phys.* **B 605** (2001) 600 [hep-ph/0102316] [INSPIRE].

[54] G. Buchalla, A.J. Buras and M.E. Lautenbacher, *Weak decays beyond leading logarithms*, *Rev. Mod. Phys.* **68** (1996) 1125 [hep-ph/9512380] [INSPIRE].

JHEP02(2019)007

[55] ETM collaboration, *B-physics from $N_f = 2$ tmQCD: the Standard Model and beyond*, *JHEP* **03** (2014) 016 [arXiv:1308.1851] [INSPIRE].

[56] Fermilab Lattice and MILC collaborations, *$B^0_{(s)}$-mixing matrix elements from lattice QCD for the Standard Model and beyond*, *Phys. Rev.* **D 93** (2016) 113016 [arXiv:1602.03560] [INSPIRE].

[57] M. Artuso, G. Borissov and A. Lenz, *CP violation in the $B^0_s$ system*, *Rev. Mod. Phys.* **88** (2016) 045002 [arXiv:1511.09466] [INSPIRE].

[58] G. Buchalla and A.J. Buras, *QCD corrections to rare K and B decays for arbitrary top quark mass*, *Nucl. Phys.* **B 400** (1993) 225 [INSPIRE].

[59] M. Misiak and J. Urban, *QCD corrections to FCNC decays mediated by Z penguins and W boxes*, *Phys. Lett.* **B 451** (1999) 161 [hep-ph/9901278] [INSPIRE].

[60] G. Buchalla and A.J. Buras, *The rare decays $K \to \pi\nu\bar{\nu}$, $B \to X\nu\bar{\nu}$ and $B \to \ell^+\ell^-$: an update*, *Nucl. Phys.* **B 548** (1999) 309 [hep-ph/9901288] [INSPIRE].

[61] C. Bobeth, M. Gorbahn and E. Stamou, *Electroweak corrections to $B_{s,d} \to \ell^+\ell^-$*, *Phys. Rev.* **D 89** (2014) 034023 [arXiv:1311.1348] [INSPIRE].

[62] T. Hermann, M. Misiak and M. Steinhauser, *Three-loop QCD corrections to $B_s \to \mu^+\mu^-$*, *JHEP* **12** (2013) 097 [arXiv:1311.1347] [INSPIRE].

[63] C. Bobeth, M. Gorbahn, T. Hermann, M. Misiak, E. Stamou and M. Steinhauser, *$B_{s,d} \to \ell^+\ell^-$ in the Standard Model with reduced theoretical uncertainty*, *Phys. Rev. Lett.* **112** (2014) 101801 [arXiv:1311.0903] [INSPIRE].

[64] X.-Q. Li, J. Lu and A. Pich, *$B^0_{s,d} \to \ell^+\ell^-$ decays in the aligned two-Higgs-doublet model*, *JHEP* **06** (2014) 022 [arXiv:1404.5865] [INSPIRE].

[65] X.-D. Cheng, Y.-D. Yang and X.-B. Yuan, *Revisiting $B_s \to \mu^+\mu^-$ in the two-Higgs doublet models with $Z_2$ symmetry*, *Eur. Phys. J.* **C 76** (2016) 151 [arXiv:1511.01829] [INSPIRE].

[66] K. De Bruyn et al., *Probing new physics via the $B^0_s \to \mu^+\mu^-$ effective lifetime*, *Phys. Rev. Lett.* **109** (2012) 041801 [arXiv:1204.1737] [INSPIRE].

[67] A.J. Buras, R. Fleischer, J. Girrbach and R. Knegjens, *Probing new physics with the $B_s \to \mu^+\mu^-$ time-dependent rate*, *JHEP* **07** (2013) 077 [arXiv:1303.3820] [INSPIRE].

[68] D. Chang, W.S. Hou and W.-Y. Keung, *Two loop contributions of flavor changing neutral Higgs bosons to $\mu \to e\gamma$*, *Phys. Rev.* **D 48** (1993) 217 [hep-ph/9302267] [INSPIRE].

[69] R. Kitano, M. Koike and Y. Okada, *Detailed calculation of lepton flavor violating muon electron conversion rate for various nuclei*, *Phys. Rev.* **D 66** (2002) 096002 [*Erratum ibid.* **D 76** (2007) 059902] [hep-ph/0203110] [INSPIRE].

[70] J.R. Ellis, K.A. Olive and C. Savage, *Hadronic uncertainties in the elastic scattering of supersymmetric dark matter*, *Phys. Rev.* **D 77** (2008) 065026 [arXiv:0801.3656] [INSPIRE].

[71] R.D. Young and A.W. Thomas, *Recent results on nucleon sigma terms in lattice QCD*, *Nucl. Phys.* **A 844** (2010) 266C [arXiv:0911.1757] [INSPIRE].

[72] T. Suzuki, D.F. Measday and J.P. Roalsvig, *Total nuclear capture rates for negative muons*, *Phys. Rev.* **C 35** (1987) 2212 [INSPIRE].

[73] M. Jung, X.-Q. Li and A. Pich, *Exclusive radiative B-meson decays within the aligned two-Higgs-doublet model*, *JHEP* **10** (2012) 063 [arXiv:1208.1251] [INSPIRE].

JHEP02(2019)007

[74] Particle Data Group collaboration, *Review of particle physics*, *Phys. Rev.* **D 98** (2018) 030001 [INSPIRE].

[75] CKMfitter Group collaboration, *CP violation and the CKM matrix: assessing the impact of the asymmetric B factories*, *Eur. Phys. J.* **C 41** (2005) 1 [hep-ph/0406184] [INSPIRE].

[76] I. Esteban, M.C. Gonzalez-Garcia, M. Maltoni, I. Martinez-Soler and T. Schwetz, *Updated fit to three neutrino mixing: exploring the accelerator-reactor complementarity*, *JHEP* **01** (2017) 087 [arXiv:1611.01514] [INSPIRE].

[77] S. Aoki et al., *Review of lattice results concerning low-energy particle physics*, *Eur. Phys. J.* **C 77** (2017) 112 [arXiv:1607.00299] [INSPIRE].

[78] HFLAV collaboration, *Averages of b-hadron, c-hadron and $\tau$-lepton properties as of summer 2016*, *Eur. Phys. J.* **C 77** (2017) 895 [arXiv:1612.07233] [INSPIRE].

[79] MEG collaboration, *Search for the lepton flavour violating decay $\mu^+ \to e^+\gamma$ with the full dataset of the MEG experiment*, *Eur. Phys. J.* **C 76** (2016) 434 [arXiv:1605.05081] [INSPIRE].

[80] SINDRUM II collaboration, *A search for muon to electron conversion in muonic gold*, *Eur. Phys. J.* **C 47** (2006) 337 [INSPIRE].

[81] ATLAS and CMS collaborations, *Measurements of the Higgs boson production and decay rates and constraints on its couplings from a combined ATLAS and CMS analysis of the LHC pp collision data at $\sqrt{s} = 7$ and 8 TeV*, *JHEP* **08** (2016) 045 [arXiv:1606.02266] [INSPIRE].

[82] LHC Higgs Cross Section Working Group collaboration, *Handbook of LHC Higgs cross sections: 3. Higgs properties*, arXiv:1307.1347 [INSPIRE].

[83] J. Bernon and B. Dumont, *Lilith: a tool for constraining new physics from Higgs measurements*, *Eur. Phys. J.* **C 75** (2015) 440 [arXiv:1502.04138] [INSPIRE].

[84] CDF and D0 collaborations, *Higgs boson studies at the Tevatron*, *Phys. Rev.* **D 88** (2013) 052014 [arXiv:1303.6346] [INSPIRE].

[85] A.J. Buras and J. Girrbach, *Towards the identification of new physics through quark flavour violating processes*, *Rept. Prog. Phys.* **77** (2014) 086201 [arXiv:1306.3775] [INSPIRE].

[86] S. Bertolini, A. Maiezza and F. Nesti, *Present and future K and B meson mixing constraints on TeV scale left-right symmetry*, *Phys. Rev.* **D 89** (2014) 095028 [arXiv:1403.7112] [INSPIRE].

[87] D. Barducci and A.J. Helmboldt, *Quark flavour-violating Higgs decays at the ILC*, *JHEP* **12** (2017) 105 [arXiv:1710.06657] [INSPIRE].

[88] MEG II collaboration, *The design of the MEG II experiment*, *Eur. Phys. J.* **C 78** (2018) 380 [arXiv:1801.04688] [INSPIRE].

[89] M. Lindner, M. Platscher and F.S. Queiroz, *A call for new physics: the muon anomalous magnetic moment and lepton flavor violation*, *Phys. Rept.* **731** (2018) 1 [arXiv:1610.06587] [INSPIRE].

JHEP02(2019)007